J Physiol 587.5 (2009) pp 1013–1032

The Journal of Physiology

Brain-derived neurotrophic factor drives the changes in excitatory synaptic transmission in the rat superficial dorsal horn that follow sciatic nerve injury

Van B. Lu[2], James E. Biggs[1,2], Martin J. Stebbing[5], Sridhar Balasubramanyan[2], Kathryn G. Todd[1,4], Aaron Y. Lai[1], William F. Colmers[1,2], David Dawbarn[6], Klaus Ballanyi[1,3] and Peter A. Smith[1,2]

[1]*Centre for Neuroscience and Departments of* [2]*Pharmacology,* [3]*Physiology and* [4]*Psychiatry, University of Alberta, Edmonton, Alberta, Canada*
[5]*School of Biomedical Sciences, RMIT University, Bundoora, Victoria, Australia*
[6]*Department of Biochemistry, University of Bristol, Bristol, UK*

Peripheral nerve injury can promote neuropathic pain. The basis of the 'central sensitization' that underlies this often intractable condition was investigated using 14–20-day chronic constriction injury (CCI) of the sciatic nerve of 20-day-old rats followed by electrophysiological analysis of acutely isolated spinal cord slices. In addition, defined-medium organotypic spinal cord slice cultures were exposed for 5–6 days to brain-derived neurotrophic factor (BDNF, 200 ng ml^{-1}) or to medium conditioned with activated microglia (aMCM). Since microglial activation is an early consequence of CCI, the latter manipulation allowed us to model the effect of peripheral nerve injury on the dorsal horn *in vitro*. Using whole-cell recording from superficial dorsal horn neurons, we found that both BDNF and CCI increased excitatory synaptic drive to putative excitatory 'radial delay' neurons and decreased synaptic excitation of inhibitory 'tonic islet/central' neurons. BDNF also attenuated synaptic excitation of putative GABAergic neurons identified by glutamic acid decarboxylase (GAD) immunoreactivity. Intrinsic neuronal properties (rheobase, input resistance and action potential discharge rates) were unaffected. Exposure of organotypic cultures to either BDNF or aMCM increased overall excitability of the dorsal horn, as seen by increased cytoplasmic Ca^{2+} responses to 35 mM K^+ as monitored by confocal Fluo-4AM imaging. The effect of aMCM was attenuated by the recombinant BDNF binding protein TrkBd5 and the effect of BDNF persisted when GABAergic inhibition was blocked with SR95531. These findings suggest that CCI enhances excitatory synaptic drive to excitatory neurons but decreases that to inhibitory neurons. Both effects are mediated by nerve injury-induced release of BDNF from microglia.

(Received 10 November 2008; accepted after revision 2 January 2009; first published online 5 January 2009)
Corresponding author P. A. Smith: Department of Pharmacology, 9.75 Medical Sciences Building, University of Alberta, Edmonton, Alberta, T6G 2H7, Canada. Email: peter.a.smith@ualberta.ca

Pain induced by injury to the nervous system often persists for months or years after the initial tissue damage has healed. This maladaptive 'neuropathic pain' serves no obvious biological purpose (Iadarola & Caudle, 1997; Treede *et al.* 2008). It contributes to morbidity associated with post-herpetic, diabetic and HIV-induced neuropathies and is associated with peripheral nerve, spinal cord and brain injuries, including stroke.

In experimental animals, chronic constriction injury (CCI) of the sciatic nerve induces pain-related behaviours that are accepted as models for human neuropathic pain (Mosconi & Kruger, 1996; Kim *et al.* 1997). These behaviours are associated with an enduring increase in the excitability of neuronal circuits of the spinal dorsal horn. This leads to the phenomenon of 'central sensitization' (Woolf, 1983; Woolf & Mannion, 1999; Dalal *et al.* 1999; Moore *et al.* 2002) that is also characteristic of human neuropathic pain. Many details of the underlying neurophysiological mechanism of 'central sensitization' remain to be elucidated. For example, little attention has been paid to the possibility that peripheral nerve injury produces differential changes in excitatory and inhibitory dorsal horn neurons (Graham *et al.* 2007; Polgar & Todd, 2008).

We have shown previously that 10–20 days of sciatic nerve chronic constriction injury (CCI) produces a characteristic 'electrophysiological signature' or pattern of changes in synaptic excitation of five different electrophysiologically defined neuronal phenotypes in the

© 2009 The Authors. Journal compilation © 2009 The Physiological Society
DOI: 10.1113/jphysiol.2008.166306

substantia gelatinosa of the rat dorsal horn. Whilst CCI increases excitatory synaptic drive to four of the five neuronal types, excitation of a large population of neurons, those that exhibit a tonic discharge pattern, is diminished (Balasubramanyan *et al.* 2006). The onset of this 'electrophysiological signature' coincides with the appearance of mechanical allodynia and hyperalgesia, two recognized behavioural signs of neuropathic pain (Balasubramanyan *et al.* 2006). CCI also activates spinal microglia (Tsuda *et al.* 2003; Tsuda *et al.* 2005; Coull *et al.* 2005) and causes them to release brain derived neurotrophic factor (BDNF). Neuropathic pain-related behaviours, are attenuated by sequestering BDNF (Yajima *et al.* 2005; Coull *et al.* 2005). Because the spinal concentration of this neurotropin is elevated for several days following injury (Cho *et al.* 1998; Dougherty *et al.* 2000), we also examined the effect of long-term exposure of spinal neurons to BDNF. These experiments, which involved the use of organotypic slice cultures, showed that 5–6 days' exposue to BDNF produces a very similar 'electrophysiological signature' to that seen with CCI. Thus, tonically firing neurons receive less excitatory synaptic drive, whereas other neuron types exhibit an increase in amplitude and/or frequency of spontaneous excitatory postsynaptic currents (sEPSCs) (Lu *et al.* 2007).

Although the relationship between firing properties, functionality and morphology of neurons in the superficial spinal laminae is a topic of continued debate (Prescott & de Koninck, 2002; Heinke *et al.* 2004; Dougherty *et al.* 2005; Santos *et al.* 2007; Maxwell *et al.* 2007) a tonic discharge pattern has been associated with inhibitory neurons (Lu & Perl, 2003; Schoffnegger *et al.* 2006). This raises the possibility that CCI selectively attenuates excitatory synaptic drive to inhibitory neurons whilst increasing excitation of other neuronal types (see Polgar & Todd, 2008). We have therefore further characterized the effects of CCI on subsets of putative excitatory and inhibitory neurons in acute slices as defined by both electrophysiological and morphological or immunocytochemical criteria. Since differential effects of CCI on different neuronal types may reflect selective actions of BDNF on excitatory and inhibitory neurons, we next examined the effect of BDNF on similarly defined groups of putative excitatory and putative inhibitory neurons in organotypic culture. To test whether BDNF may be *responsible* for the effects seen with CCI, we used confocal imaging to measure the cystolic Ca^{2+} response of groups of individual neurons to a high K^+ challenge. An increase in the response was taken to imply an increase in overall dorsal horn excitability. Since activation of spinal microglia is one of the early consequences of CCI (Coull *et al.* 2005), we also applied a medium that was preconditioned by exposure to activated microglia (aMCM) to mimick, in organotypic culture, the effect of CCI *in vivo*. The recombinant BDNF binding protein TrkBd5 (Banfield *et al.* 2001) was used to test whether the presence of microglial-derived BDNF can account for the changes in excitability seen with aMCM and hence with those associated with CCI.

Methods

Surgery and acute slice preparation

All procedures complied with the guidelines of the Canadian Council for Animal Care and the University of Alberta Health Sciences Laboratory Animal Services Welfare Committee.

The left sciatic nerve of 20-day-old male Sprague–Dawley rats was subjected to chronic constriction injury (CCI) using two 2 mm long polyethylene cuffs fashioned from PE90 tubing and applied to enclose the nerve (Mosconi & Kruger, 1996). The nerve was exposed at mid-thigh level under isoflourane anaesthesia. Sham surgery was carried out on 45 animals in which the sciatic nerve was exposed but not deliberately manipulated. All neurons recorded in animals subject to CCI were obtained from a cohort of 46 rats that exhibited mechanical hyperalgesia and allodynia as assessed with von Frey filaments (Balasubramanyan *et al.* 2006). Ten to twenty days after surgery, rats were anaesthetized with an overdose of intraperitoneal urethane ($1.5\,g\,kg^{-1}$). Laminectomy was performed after the cessation of respiration and complete loss of ocular and nociceptive reflexes. The entire spinal cord, from the sacral to cervical region, was removed. Cardiac ventricles were punctured with scissors prior to animal disposal. The thoracic cord was cut into 300 μm transverse slices using a vibrating microtome. Detailed methods for slice preparation and recording from substantia gelatinosa neurons, ipsilateral to the injury in 30- to 45-day-old rats were as previously described (Balasubramanyan *et al.* 2006; Moran *et al.* 2004). Dissection solution contained (in mM): 118 NaCl, 2.5 KCl, 26 $NaHCO_3$, 1.3 $MgSO_4$, 1.2 NaH_2PO_4, 1.5 $CaCl_2$, 5 $MgCl_2$, 25 D-glucose, 1 kynurenic acid, continuously bubbled with 95% O_2–5% CO_2. Slices were equilibrated for 1 h at 37°C in dissection solution without kynurenic acid prior to recording but were subsequently stored at room temperature.

Organotypic cultures

Neurons were allowed to develop in organotypic culture for 21–35 days so that their age on exposure to BDNF was similar to the age of *in vivo* neurons in animals subject to sciatic CCI (Lu *et al.* 2007). Cultures were made from E13–14 rats as previously described (Lu *et al.* 2006). Briefly, rat fetuses were delivered by caesarean section from timed-pregnant Sprague–Dawley dams under isoflurane anaesthesia. The dam was subsequently killed

© 2009 The Authors. Journal compilation © 2009 The Physiological Society

with an overdose of intracardial chloral hydrate (10.5%). The entire embryonic sac was placed in chilled Hanks' balanced salt solution containing (in mM): 138 NaCl, 5.33 KCl, 0.44 KH_2PO_4, 0.5 $MgCl_2$–$6H_2O$, 0.41 $MgSO_4$–$7H_2O$, 4 $NaHCO_3$, 0.3 Na_2HPO_4, 5.6 D-glucose and 1.26 $CaCl_2$. Individual rat fetuses were removed from their embryonic sacs and rapidly decapitated. The spinal cord from each fetus was isolated in the above solution and sliced into 275–325 μm transverse slices using a McIlwain tissue chopper. Only lumbar cord slices with two attached dorsal root ganglia were chosen. These were trimmed of excess ventral tissue and allowed to recover for 1 h at 4°C. Each slice was then attached to a coverslip with a clot of reconstituted chicken plasma and thrombin. Coverslips were placed in 1 ml medium containing 82% Dulbecco's modified Eagle's medium (DMEM), 10% fetal bovine serum (FBS) and 8% sterile water in flat-bottomed culture tubes. These were placed into a roller drum rotating at 120 rotations per hour in a dry heat incubator at 36°C. Medium was supplemented with 20 ng ml^{-1} nerve growth factor (NGF, Alomone Laboratories, Jerusalem, Israel) for the first 4 days, and omitted thereafter. Antibiotic and antimycotic drugs (5 units ml^{-1} penicillin G, 5 units ml^{-1} streptomycin and 12.5 ng ml^{-1} amphotericin B; Gibco) were also included in the media during the first 4 days of culture. After this, slices were treated with an antimitotic drug cocktail consisting of uridine, cytosine-β-D-arabino-furanoside (AraC), and 5-fluorodeoxyuridine (all at 10 μM) for 24 h to impair the overgrowth of glial cells. During antimitotic treatment, the serum medium was progressively switched (first diluted 50 : 50 after 4 days, then completely exchanged after 5 days) to a defined, neurotrophin- and serum-free medium consisting of Neurobasal medium with N-2 supplement and 5 mM Glutamax-1 (all from Gibco). The medium within these tubes was exchanged regularly with freshly prepared medium every 3–4 days.

Microglia-conditioned medium

Methods for microglia isolation were adapted from Siao & Tsirka (2002). Whole brains of postnatal day 1 Sprague–Dawley rats were dissected in Hanks' balanced salt solution without divalent ions to prepare mixed glial cultures. Brains were dissociated by 15 min enzymatic digestion with 0.25% trypsin-EDTA followed by mechanical titrations in DMEM/F-12 containing 10% FBS. Poly L-lysine-coated 100 mm dishes were used to plate out the mixed glia in DMEM/F-12 with 10% FBS at a density of 8×10^6 cells per dish. After 8–14 days of culture, 15 mM lidocaine was added for 5 min to inhibit adhesion molecules. Cultures were shaken on a rotator at 100 r.p.m. for 30 min. The medium was collected and centrifuged at 2000 *g* for 5 min. The supernatant was discarded and the pellet was resuspended in DMEM and plated into 24-well tissue culture plates. After 45 min incubation, microglia were washed with DMEM twice to remove non-adhering cells. After 24 h incubation half of the microglia culture was activated with 100 ng ml^{-1} lipopolysacharide (LPS) for 6 h, the other half of the microglia received phosphate buffered saline (PBS). LPS was removed after 6 h with 3 PBS washes and then replaced with 'Neurobasal' culture medium. After 24 h, medium was harvested and used to culture 14–21 days organotypic spinal cord slices.

Recording and data analysis

For recording, acute slices or organotypically cultured slices were superfused at ~22°C with 95% O_2–5% CO_2 saturated aCSF which contained (in mM): 127 NaCl, 2.5 KCl, 1.2 NaH_2PO_4, 26 $NaHCO_3$, 1.3 $MgSO_4$, 2.5 $CaCl_2$, 25 D-glucose, pH 7.4. In acute slices, the two substantiae gelatinosae appeared as translucent bands under infrared differential-interference optics and neurons were patched under visual control. The region was less well defined in the organotypic cultures and recordings were made 0.5–2 mm from the dorsal surface. Recording pipettes (DC resistance 5–10 MΩ) were filled with a solution containing (in mM): 130 potassium gluconate, 1 $MgCl_2$, 2 $CaCl_2$, 10 Hepes, 10 EGTA, 4 Mg-ATP, 0.3 Na-GTP, pH 7.2, 290–300 mosmol l^{-1}.

Recordings were made using an NPI SEC-05LX amplifier (ALA Scientific Instruments, Westbury, NY, USA) in bridge balance or in discontinuous, single electrode, current or voltage-clamp mode. Current was injected to polarize neuronal membrane potential to −60 mV prior to applying additional depolarizing 800 ms current pulses to determine rheobase and to study the pattern of action potential discharge (Balasubramanyan *et al.* 2006). Membrane excitability was assessed by measuring the cumulative latency of action potentials in response to depolarizing current ramps at 33, 67, 100 or 133 pA s^{-1}. Data were acquired and analysed using pCLAMP 8.0 or 9.0 (Axon Instruments/Molecular Devices, Sunnyvale, CA, USA).

As in our previous studies (Lu *et al.* 2006; Lu *et al.* 2007), Mini Analysis Program (Synaptosoft, Decatur, GA, USA) was used to distinguish sEPSCs from baseline noise. Events were detected automatically by setting appropriate amplitude and area threshold for each neuron. All events detected during a 3 min acquisition period were then re-examined and visually accepted or rejected based on subjective visual examination (Moran *et al.* 2004). All available events were used to calculate mean interevent intervals and mean sEPSC amplitude (Tables 1–3). Amplitude and interevent intervals were also compared using cumulative distribution plots and the Kolmogorov-Smirnov two-sample test. Data from the full 3 min data records were analysed for neurons in acute slices

© 2009 The Authors. Journal compilation © 2009 The Physiological Society

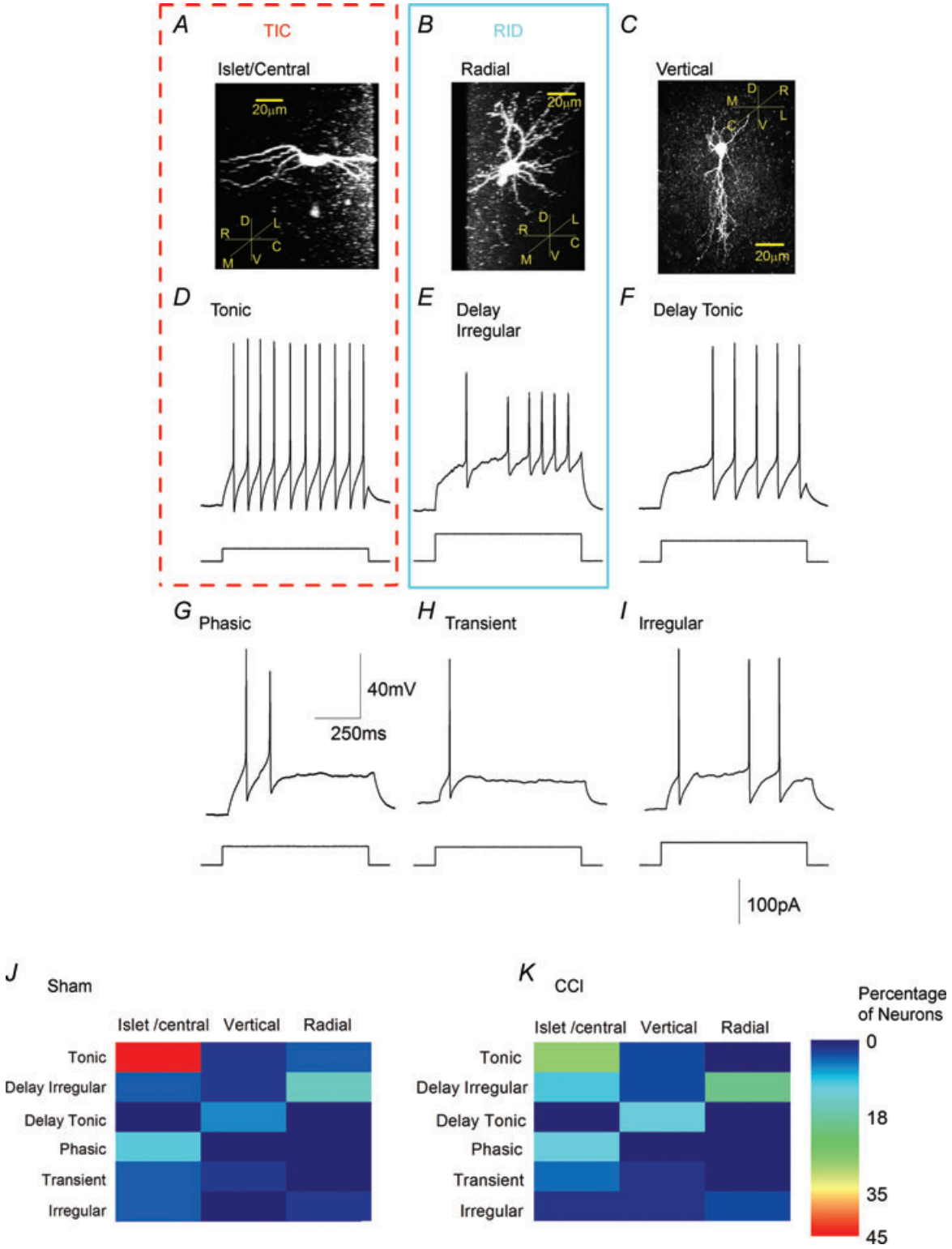

Figure 1. Morphologically and electrophysiologically defined neuronal phenotypes in acutely isolated substantia gelatinosa slices

A–C, confocal images of biocytin-filled neurons; insets illustrate directions of rostrocaudal (R,C), mediolateral (M,L) and dorsoventral (D,V) planes; dashed line drawn at 45 deg represents plane in and out of page. *A*, islet/central neuron; note overall bipolar appearance and rostrocaudal projection of dendritic tree. *B*, radial cell. *C*, vertical neuron with characteristic dorsoventral dendritic projection. *D–I*, characteristic discharge patterns of tonic, delay irregular, delay tonic, phasic, transient and irregular neurons evoked by depolarizing current commands evoked

© 2009 The Authors. Journal compilation © 2009 The Physiological Society

(Fig. 2*D*, *E*, *G* and *H*) whereas the first 100 events after the first minute of recording were analysed for neurons in organotypic culture (Figs 4*D*, *E*, *G* and *H* and 6*F–I*). This was because the frequency of spontaneous synaptic events was typically much higher in the cultures (Lu *et al.* 2006) and we wished to consider similar sample sizes when comparing control and experimental data.

Morphological and immunocytochemical analysis

Recorded neurons were filled with biocytin (0.2%) and slices fixed in cold (4°C) 4% paraformaldehyde in PBS (Balasubramanyan *et al.* 2006). Slices were rinsed and stained by incubating with 0.3% Triton X-100 and streptavidin-Texas red conjugate (1 : 50 dilution, Molecular Probes, Eugene, OR, USA). They were then rinsed with distilled water, transferred to slides, allowed to dry overnight and coverslipped with Cytoseal^{TM}-60 (Richard-Allan Scientific, Kalamazoo, MI, USA). A Bio-Rad MRC1024 confocal laser scanning system, installed on a Zeiss Axioplan 2 microscope, was used to examine acute slices. It was equipped with a krypton–argon laser and Texas red filter (wavelength 568 nm), as well as a transmitted light detector that was used to simultaneously acquire dark field images. Orientation of neurons was assessed by performing 3-D reconstructions of confocal Z-stacks. To identify GABAergic dorsal horn neurons in cultures, primary GAD antibodies (1 : 8000, anti-GAD, rabbit; Chemicon, Temecula, CA, USA) in 2% normal goat serum (NGS; Rockland, Gilbertsville, PA, USA) and 0.3% Triton X-100 solution in PBS were incubated with organotypic slices for 48 h at 4°C. Secondary antibodies (1 : 300, anti-rabbit Alexa-488; Molecular Probes, Eugene, OR, USA) in 2% NGS and 0.3% Triton X-100 in PBS were applied for 2.5 h. Texas red–streptavidin conjugate used to stain biocytin-filled cells was added after 2 h of the start of incubation with the secondary antibody solution. The concentration of antibodies was optimized using control slices to produce sufficient staining and reduce background. The fluorescent dyes used, Texas red and Alexa-488, did not produce spectral crossover in staining controls (data not shown). To visualize neuronal staining in organotypic cultures, a Zeiss inverted confocal laser scanning microscope (LSM 510; Zeiss, Toronto, ON, Canada) equipped with appropriate lasers (HeNe1, 543 nm; Argon, 488 nm) and filters was used to examine the tissue. Fluorescence confocal images and 3D reconstructions were acquired using Zeiss LSM 510 imaging software (Zeiss LSM image browser, v. 3, 2, 70).

Calcium imaging

Organotypic slice cultures treated with 5 μM Fluo-4 acetoxymethyl ester (Fluo-4-AM) were imaged as previously described (Ruangkittisakul *et al.* 2006; Lu *et al.* 2007). Changes in Ca^{2+}-fluorescence intensity evoked by a high K^+ solution (35 mM, 90 s application) were measured using a confocal microscope equipped with an argon (488 nm) laser and filters (20× XLUMPlanF1, NA 0.95 objective; Olympus FV300, Markham, Ontario, Canada). Full frame images (512 × 512 pixels) were acquired at a scanning time of 1.08 s per frame. Selected regions of interest were drawn around distinct cell bodies and traces of time course of change of fluorescence intensity were generated with FluoView v.4.3 (Olympus). Data were only collected from cells in the plane of focus that responded reversibly to a high K^+ challenge. Data were collected from 4–10 neurons in each organoypic slice.

Drugs and chemicals

BDNF was from Alomone Laboratories (Jerusalem, Isreal), SR95531, dihydrokainate (DHK), 6-Cyano-7-nitroquinoxaline-2,3-dione (CNQX) and D-(–)-2-amino-5-phosphonopentanoic acid (AP-5) (Tocris) were purchased from Cedarlane Laboratories (Hornby, Ontario, Canada). Unless otherwise stated, all other drugs and chemicals were from Sigma (St Louis, MO, USA). TrkB-d5 was prepared as previously described (Banfield *et al.* 2001).

Results

Characterization of substantia gelatinosa neurons

To examine the effect of CCI on discrete neuronal populations, cells in acutely isolated slices were characterized according to both morphological and electrophysiological criteria. Recognized morphological phenotypes include islet/central neurons that are orientated rostrocaudally (Fig. 1*A*), radial neurons that

from a resting potential set at −60 mV (Balasubramanyan *et al.* 2006). Voltage and time calibration in *G* and current amplitude calibration in *I* refer to all records. *J* and *K*, representation of coincidence of morphological and electrophysiological phenotypes in 48 neurons from sham animals and 68 neurons from animals subject to sciatic chronic constriction (CCI). Percentage of neurons in each category is represented by the false colour scale at right. Thus, tonic firing neurons with an islet/central morphology (TIC neurons) account for 45% of the neuronal population in sham animals and for 28% in CCI animals. Radial neurons which display irregular delay discharge (RID neurons) represent a second major population. Other large populations include vertical cells that exhibit a tonic delay discharge pattern as well as islet central neurons that exhibit a phasic discharge pattern. Coloured boxes drawn around *A* and *D* and B and *E* summarize the properties of TIC and RID neurons, respectively.

© 2009 The Authors. Journal compilation © 2009 The Physiological Society

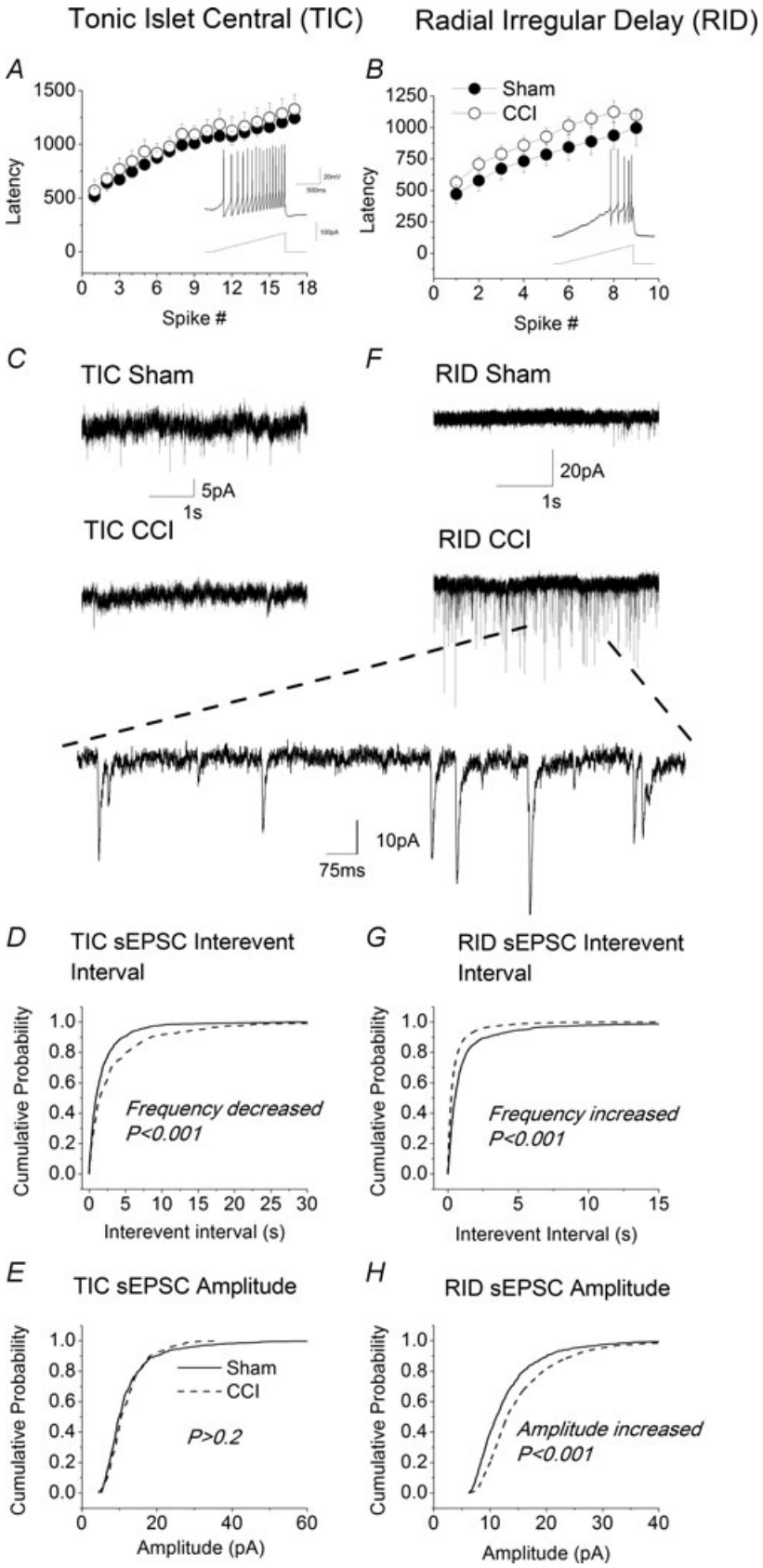

Figure 2. Effects of sciatic chronic constriction (CCI) on tonic islet/central (TIC) and radial irregular delay (RID) neurons in acute slices
A and *B*, lack of effect of CCI on excitability of TIC and RID cells, respectively. Excitability was assessed as shown in the insets by measuring the cumulative latency to the first and subsequent spikes in response to a depolarizing current ramp of 67 pA s^{-1}. Data obtained from sham operated animals (●) are not statistically different from those obtained from animals subject to CCI (○). For TIC cells, $n = 8$ for sham and $n = 7$ for CCI; for RID cells $n = 7$ for sham and $n = 4$ for CCI. *C*, sample recordings of sEPSCs in TIC neurons from sham operated (upper trace) and CCI animals (lower trace). Note decreased activity in CCI neurons. *D* and *E*, cumulative probability plots for effects of CCI on interevent interval (IEI) and amplitude and of sEPSCs in TIC neurons. For TIC neurons; 626 events were analysed from slices in sham operated animals ($n = 13$ neurons) and 341 events from CCI animals ($n = 14$ neurons). *F*, sample recordings of sEPSC in RID neurons from slices from sham-operated (upper trace) and CCI animals (lower trace). Note CCI-induced increase in synaptic activity in RID neurons. Large inset is sampling of recording in lower trace on a fast time scale. *G* and *H*, cumulative probability plots for effects of CCI on IEI and amplitude of sEPSCs in RID neurons. Events analysed from 'RID' neurons; 1074 (sham) ($n = 12$ neurons), 3746 (CCI) ($n = 17$ neurons). *P*-values derived from Kolmogorov–Smirnov test are indicated on graphs.

© 2009 The Authors. Journal compilation © 2009 The Physiological Society

Table 1. Effect of chronic constriction injury (CCI) on electrophysiological properties of tonic islet/central neurons (TIC) and radial irregular-delay (RID) neurons

	Tonic islet central neurons (TIC)	Radial irregular delay neurons (RID)
RMP sham (mV)	-57.4 ± 2.2 ($n = 25$)	-53.6 ± 2.1 ($n = 17$)
RMP CCI (mV)	-56.5 ± 2.2 ($n = 17$; $P > 0.7$)	-53.6 ± 2.5 ($n = 14$; $P > 0.99$)
Rheobase sham (pA)	21.7 ± 2.7 ($n = 17$)	98.0 ± 15.2 ($n = 12$)
Rheobase CCI (pA)	27.6 ± 2.2 ($n = 19$; $P = 0.09$)	89.0 ± 10.0 ($n = 13$: $P > 0.6$)
Input resistance sham (MΩ)	762 ± 141 ($n = 13$)	442 ± 123 ($n = 10$)
Input resistance CCI (MΩ)	662 ± 124 ($n = 11$ $P = 0.3$)	472 ± 73 ($n = 11$ $P > 0.5$)
sEPSC		
IEI sham (ms)	1989 ± 138 ($n = 626$ events from 13 neurons)	1487 ± 146 ($n = 1074$ events from 12 neurons)
IEI CCI (ms)	3678 ± 360 ($n = 342$ events from 14 neurons; $P < 0.001$)	590 ± 23 ($n = 3746$ events from 17 neurons; $P < 0.001$))
Amplitude sham (pA)	12.8 ± 0.7 ($n = 747$ events from 13 neurons)	13.0 ± 0.2 ($n = 1076$ events from 12 neurons))
Amplitude CCI (pA)	11.9 ± 0.2 ($n = 488$ from 14 neurons; $P > 0.3$)	15.3 ± 0.1 ($n = 3763$ events from 17 neurons; $P < 0.001$)

Data expressed as means ± S.E.M. *P*-values refer to comparison of data from sham and CCI groups. RMP, resting membrane potential; IEI, interevent interval. sEPSC statistics obtained from all events occurring within a 3 min recording period.

send processes in all directions (Fig. 1*B*) and vertical neurons that are orientated dorsoventrally (Fig. 1*C*) (Gobel, 1978; Grudt & Perl, 2002). The horizontal plane of section that we used made it very difficult to distinguish between central and islet cells as both exhibit major rostrocaudal projections (Grudt & Perl, 2002). Analysis of electrophysiological phenotype identified six prevalent firing patterns. As in our previous studies (Balasubramanyan *et al.* 2006), these included neurons with 'tonic' (Fig. 1*D*), 'phasic' (Fig. 1*G*), 'transient' (Fig. 1*H*) or 'irregular' (Fig. 1*I*) discharge patterns. However, the previously defined 'delay' phenotype (Balasubramanyan *et al.* 2006) appeared to fall into two separate categories. 'Delay irregular' neurons, which exhibited an irregular discharge of low amplitude action potentials after an initial delay (Fig. 1*E*) and 'delay-tonic' neurons (Fig. 1*F*) which after an initial delay, discharged with regularly spaced, high amplitude action potentials.

Comparison of the morphologies and firing patterns of control substantia gelatinosa neurons from sham-operated animals revealed that there was no absolute correlation between firing pattern and morphology (Fig. 1*J*). Nevertheless, certain trends and discrete populations could be identified. For example, we found that 45% of all control neurons exhibited both islet/central cell morphology (Fig. 1*A*) *and* a 'tonic' discharge pattern (Fig. 1*D*). Since both a tonic firing pattern (Lu & Perl, 2003) and an islet cell morphology (Todd & Spike, 1993; Lu & Perl, 2003; Heinke *et al.* 2004; Maxwell *et al.* 2007) have been associated with GABAergic and/or glycinergic function, tonic islet/central neurons (TIC neurons), which exhibit both of these characteristics, are very likely to be inhibitory. Another 14% of neurons exhibited a radial morphology (Fig. 1*B*) associated with the delayed irregular discharge pattern (Fig. 1*E*). Since neurons exhibiting a delayed discharge pattern rarely exhibit a GABAergic phenotype (Heinke *et al.* 2004; Schoffnegger *et al.* 2006) and generate EPSPs when stimulated in paired recording experiments (Lu & Perl, 2005), radial irregular delay cells (RID) neurons are likely to be excitatory interneurons.

Other populations included vertical neurons (Fig. 1*C*) that exhibited a tonic delay discharge pattern (Fig. 1*F*) but these were excluded from further analysis as they accounted for only 6% of the total neuronal population in the control situation. Another 10% of the population comprised islet/central neurons (Fig. 1*A*) that exhibited a phasic discharge pattern (Fig. 1*G*). These too were excluded as central cells with a phasic discharge pattern

© 2009 The Authors. Journal compilation © 2009 The Physiological Society

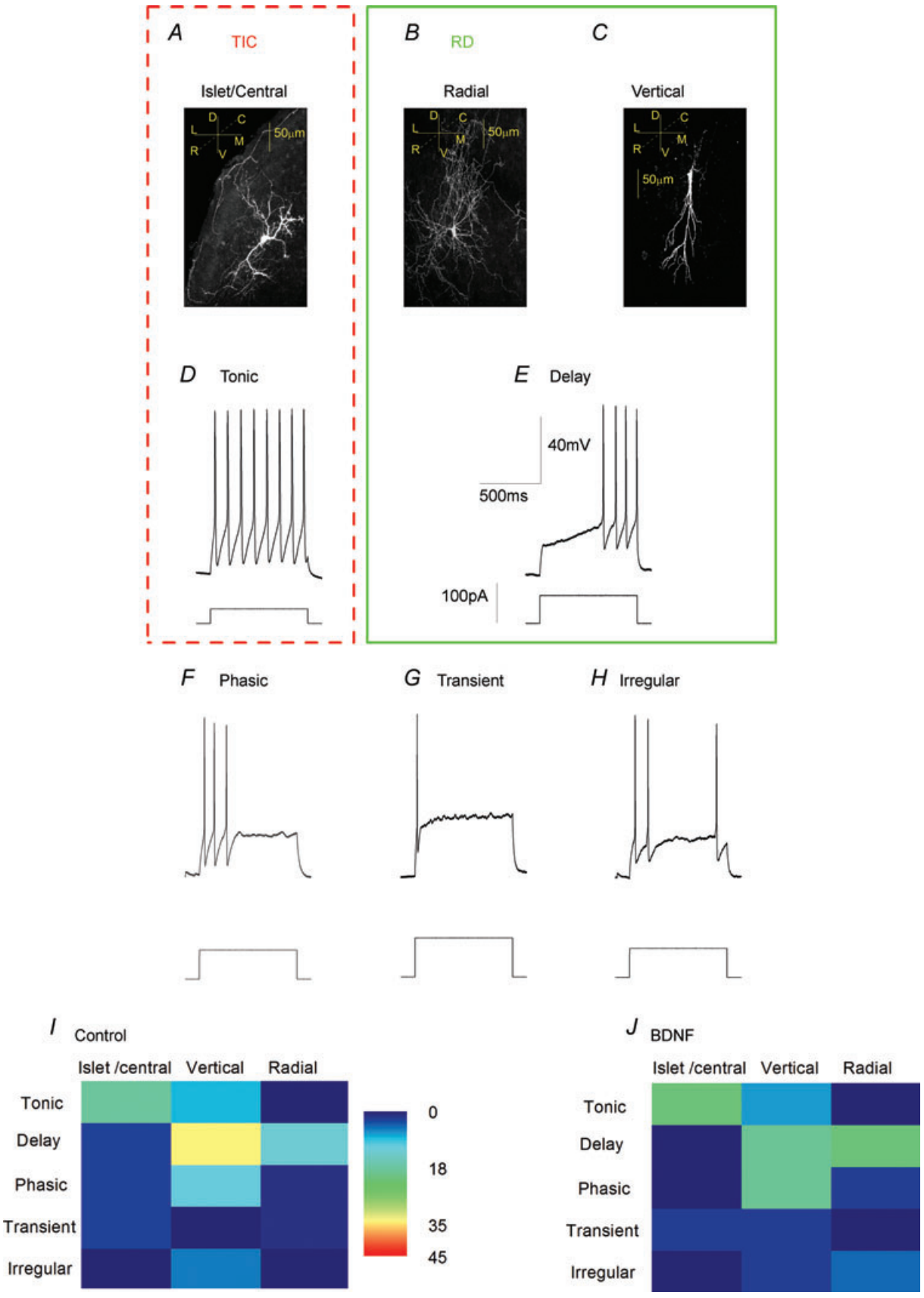

© 2009 The Authors. Journal compilation © 2009 The Physiological Society

have been reported to behave as excitatory interneurons (Lu & Perl, 2005) whereas islet cells with a phasic discharge pattern may be inhibitory (Heinke *et al.* 2004). Thus, the phasic islet/central population of neurons was likely to have comprised a mixture of excitatory and inhibitory neurons that would be unsuitable for testing our hypothesis that CCI increases excitatory drive to excitatory neurons whilst compromising that to inhibitory neurons. We therefore confined our examination of the effect of sciatic CCI to RID and TIC neurons.

CCI increases excitatory synaptic drive to putative excitatory neurons and decreases it to putative inhibitory neurons

Large populations of TIC and RID neurons persisted after injury that represented 28% and 20% of the total cell population, respectively (Fig. 1*K*). Although the resting membrane potential, rheobase and excitability of TIC and RID cells were unaffected after 14–20 days of CCI (Fig. 2*A* and *B*; see Table 1) there were obvious changes in excitatory synaptic transmission that were specific to neuron type. Thus, sEPSC frequency in TIC neurons was significantly decreased (IEI increased, Fig. 2*C–E*, Table 1) whereas there was a significant increase in both the frequency and amplitude of sEPSCs in putative excitatory RID neurons (Fig. 2*F–H*, Table 1). These changes were significant according to both the Kolmogorov–Smirnov test (Fig. 2*F–H*) and comparison of mean amplitudes and interevent intervals using Student's unpaired *t* test (Table 1).

BDNF *in vitro* mimics the effect of CCI *in vivo*

It is now well accepted that BDNF (Tsuda *et al.* 2003; Tsuda *et al.* 2005; Coull *et al.* 2005) is a major instigator of the altered dorsal horn excitability that accompanies peripheral nerve injury (Thompson *et al.* 1999; Groth & Aanonsen, 2002; Garraway *et al.* 2003). The similarity between the 'electrophysiological signature' produced by CCI (Balasubramanyan *et al.* 2006) *in vivo* and that produced by BDNF (Lu *et al.* 2007) in organotypic culture prompted us to examine whether BDNF also produced increased excitatory drive to RID neurons and attenuated excitation of TIC neurons in a similar fashion to CCI (Fig. 2).

We and others have previously noted a remarkable physiological and developmental similarity between rodent spinal cord neurons in organotypic culture and those of a similar age in intact animals (Avossa *et al.* 2003; Lu *et al.* 2006). In agreement with this, Fig. 3*A–C* shows that islet/central, radial and vertical cells could also be identified in organotypic slice cultures. Although tonic, phasic, irregular and transient firing patterns were seen, delay irregular cells were not seen in the cultures (Fig. 3*D–H*) and both vertical and radial cells appeared to discharge with a delay tonic pattern (Fig. 3*I*). We therefore used data from radial delay (RD) neurons in organotypic culture for comparison with radial irregular delay (RID) neurons in acute slices (see discussion). These RD cells made up 12% of the total population of neurons in control cultures. As with acute slices, the tonic discharge pattern was frequently associated with central/islet neurons in culture (18% of total population of control neurons; Fig. 3*I*). These relationships between morphology and electrophysiological phenotype persisted when the organotypic cultures were treated with BDNF for 5–6 days. Thus 21% of neurons studied in the BDNF group exhibited the tonic islet/central (TIC) phenotype and 19% exhibited a radial delay (RD) phenotype (Fig. 3*J*).

As with CCI *in vivo* (Fig. 2), the resting membrane potential, rheobase and excitability of TIC and RD neurons in organotypic culture were unaffected by BDNF (Fig. 4*A* and *B*; see Table 2). There were, however, obvious, phenotype-specific changes in excitatory synaptic transmission that were similar to those seen after CCI (Fig. 2). Specifically, the frequency and amplitude of sEPSC in TIC cells were reduced by BDNF (Fig. 4*C–E*) whereas both the frequency and amplitude of sEPSCs in RD cells was increased (Fig. 4*F–H*). These changes were significant according to both the Kolmogorov–Smirnov test (Fig. 4*D*, *E*, *G* and *H*) and comparison of mean amplitudes and interevent intervals by means of Student's *t* test (Table 2).

Figure 3. Morphologically and electrophysiologically defined neuronal phenotypes in the superficial dorsal horn of organotypic spinal cord slices
A–C, confocal images of biocytin-filled neurons; insets illustrate anatomical co-ordinates; rostrocaudal (R,C), mediolateral (M,L) and dorsoventral (D,V) planes; dashed line drawn at 45 deg represents plane in and out of page. *A*, islet/central neuron; note overall bipolar appearance and rostrocaudal projection of dendritic tree. *B*, radial cell. *C*, vertical neuron with characteristic dorsoventral dendritic projection. *D–H*, characteristic discharge patterns of tonic, delay, phasic, transient and irregular neurons evoked by depolarizing current commands evoked from a resting potential set at −60 mV (Balasubramanyan *et al.* 2006). Voltage, current and time calibrations in *E* refer to all records. *I* and *J*, representation of coincidence of morphological and electrophysiological phenotypes in 73 neurons from slices in control organotypic cultures and 43 neurons from cultures treated with BDNF (200 ng ml^{-1}) for 5–6 days. Percentage of neurons in each category are represented by the false colour scale in *I*. Thus, tonic firing neurons with an islet/central morphology (TIC neurons) account for a large proportion of the neuronal population in both control and BDNF-treated slices.

© 2009 The Authors. Journal compilation © 2009 The Physiological Society

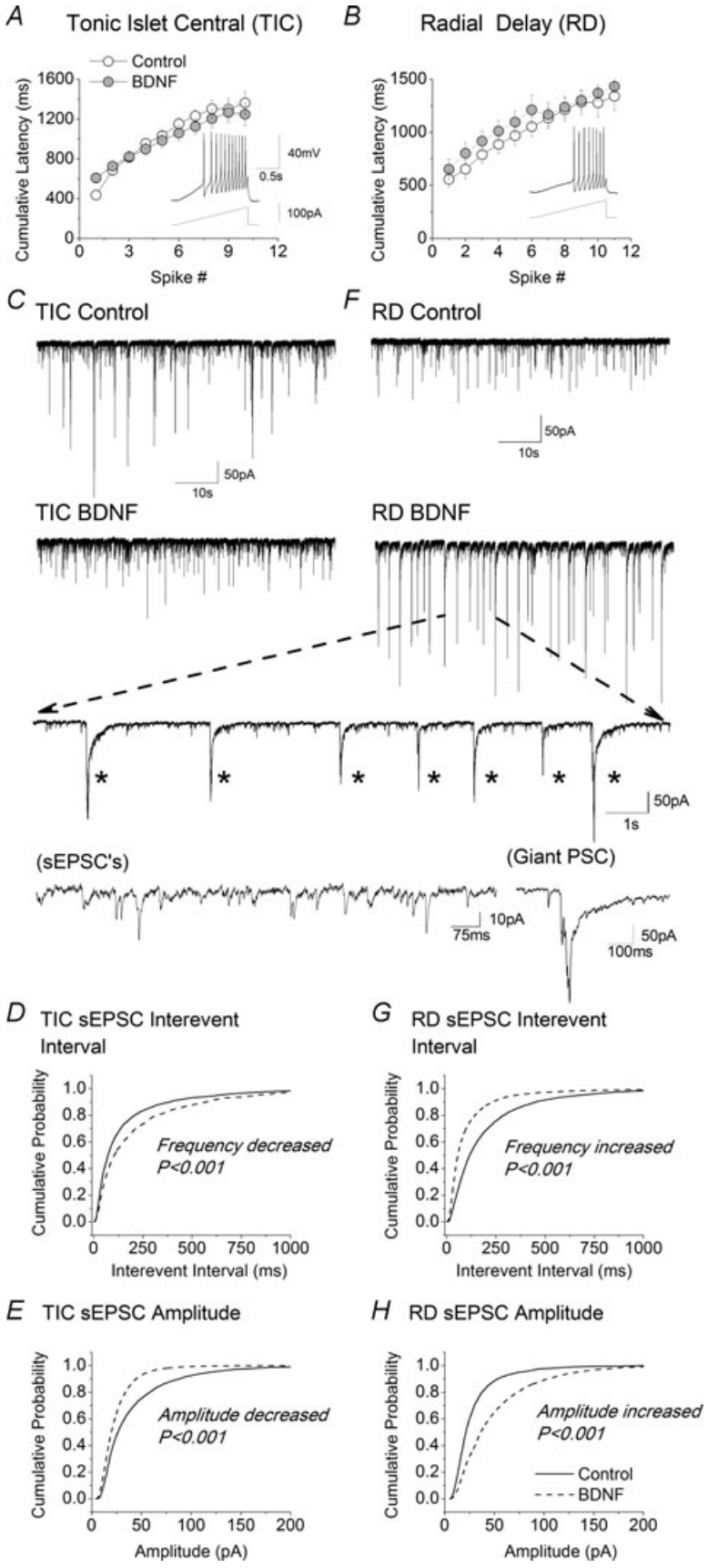

Figure 4. Effects of BDNF on tonic islet/central (TIC) and radial delay (RD) neurons in organotypic slices
A and *B*, lack of effect of BDNF on excitability of TIC and RD cells, respectively. Excitability was assessed as shown in the insets by measuring the cumulative latency to the first and subsequent spikes in response to a depolarizing current ramp of 67 pA s^{-1}. Data obtained from control neurons (○) are not statistically different from those obtained from neurons exposed to BDNF (grey circles). Control data from 8 TIC neurons and 9 RD neurons; BDNF data from 6 TIC neurons and 7 RD neurons. *C*, sample recordings of spontaneous synaptic activity at −70 mV in TIC neurons from a control organotypic slice culture (upper trace) and from one exposed to 200 ng ml^{-1} BDNF for 6 days. Note decreased activity in BDNF treated neuron. *D* and *E*, cumulative probability plots for effects of BDNF on interevent interval (IEI) and amplitude of spontaneous EPSCs (sEPSC) in TIC neurons. Data for all plots were obtained from the first 100 events following the first minute of recording from 12 TIC neurons in both the absence and the presence of BDNF. *F*, sample recordings of spontaneous synaptic activity at −70 mV in RD neurons from control (upper trace) and BDNF treated slices (lower trace). Note BDNF-induced increase in synaptic activity in RD neurons. Large inset is sampling of recording in lower trace on a fast time scale. Note presence of 'giant' postsynaptic potentials (giant 'PSP's indicated by asterisks). The amplitudes and durations of *bona fide* sEPSCs and 'giant' PSCs are compared in the lower portion of the inset. *G* and *H*, cumulative probability plots for effects of BDNF on IEI and amplitude of sEPSCs in RD neurons. Data for all plots were obtained from the first 100 events following the first minute of recording from 14 RD neurons both in the absence and presence of BDNF.

© 2009 The Authors. Journal compilation © 2009 The Physiological Society

Table 2. Effect of BDNF on electrophysiological properties of tonic islet/central neurons (TIC) and radial irregular-delay (RID) neurons

	Tonic islet central neurons (TIC)	Radial delay neurons (RD)
RMP control (mV)	-52.9 ± 4.2 ($n = 8$)	-41.8 ± 3.7 ($n = 8$)
RMP BDNF (mV)	-49.0 ± 3.9 ($n = 6$; $P > 0.5$)	-45.6 ± 0.8 ($n = 7$; $P > 0.3$)
Rheobase control (pA)	39.4 ± 10.8 ($n = 8$)	44.4 ± 8.6 ($n = 9$)
Rheobase BDNF (pA)	34.2 ± 8.4 ($n = 6$; $P > 0.7$)	72.8 ± 23.9 ($n = 7$; $P > 0.2$)
Input Resistance control (MΩ)	386 ± 83 ($n = 7$)	426 ± 78 ($n = 9$)
Input Resistance BDNF (MΩ)	370 ± 49 ($n = 6$; $P > 0.8$)	452 ± 116 ($n = 7$; $P > 0.8$)
sEPSC		
IEI control (ms)	156.2 ± 3.5 ($n = 4532$ events from 12 neurons)	198.8 ± 3.7 ($n = 4158$ events from 14 neurons)
IEI BDNF (ms)	220.5 ± 8.4 ($n = 1298$ events from 12 neurons; $P < 0.001$)	108.5 ± 2.0 ($n = 7652$ events from 14 neurons; $P < 0.001$)
Amplitude control (pA)	40.7 ± 0.55 ($n = 5626$ events from 12 neurons)	28.8 ± 0.43 ($n = 4165$ events from 14 neurons)
Amplitude BDNF (pA)	24.7 ± 0.22 ($n = 6282$ events from 12 neurons; $P < 0.001$)	49.4 ± 0.46 ($n = 7635$ events from 14 neurons; $P < 0.001$)

Data expressed as means ± S.E.M. *P*-values refer to comparison of data from control and BDNF treated groups. RMP, resting membrane potential; IEI, interevent interval. sEPSC statistics obtained from all events occurring within a 3 min recording period.

We have noted previously that the amplitude and frequency of sEPSCs in neurons in organotypic culture are far greater than those in acutely isolated slices (Lu *et al.* 2006). The large and frequent sEPSCs seen in the cultures appear to summate to produce large, slowly decaying events that we refer to as 'giant postsynaptic currents' (giant PSCs). These are marked by asterisks in the inset to Fig. 4*F*. A further expansion of the time scale of spontaneous synaptic events is also illustrated. This shows the difference between the amplitude and time course of 'regular' sEPSCs and summated giant PSCs. Since the purpose of the present study is to compare changes in sEPSCs in acute slices and organotypic cultures, the giant PSCs, which occur only in the cultures, have not been analysed further. The cumulative probability plots shown in Fig. 4*D*, *E*, *G* and *H* were derived from 'regular' sEPSCs.

The overall similarity between the effects of CCI *in vivo* and BDNF *in vitro* on TIC and RID/RD cells are summarized in Fig. 5. Figure 5*A* and *B* shows the mean interevent interval (IEI) of sEPSCs in TIC and RID/RD neurons, respectively. Both BDNF and CCI increase IEI (decrease sEPSC frequency) in TIC neurons and both decrease it (increase sEPSC frequency) in RD/RID neurons. Percentage changes in IEI in TIC and RID/RD neurons are replotted in Fig. 5*C*. Figure 5*D–F* shows similar comparisons for sEPSC amplitude. BDNF decreased sEPSC amplitude in TIC cells and both BDNF and CCI increased sEPSC amplitude in RID cells. Although BDNF reduced sEPSC amplitude in TIC cells, the effect of CCI on this population was not statistically significant (Fig. 5*D* and *F* see also Fig. 2*E* and Table 1).

BDNF decreases synaptic drive to GABAergic neurons and increases that to non-GABAergic neurons

To test further the idea that prolonged exposure to BDNF increases excitatory synaptic drive to excitatory neurons whilst decreasing that to GABAergic inhibitory neurons, we compared its actions on synaptic excitation of neurons identified *post hoc* as either glutamic acid decarboxylase (GAD) positive (GAD+) or GAD negative (GAD−). Figure 6*A* and *B* shows confocal images of the same double-labelled neuron. Its morphology was revealed using biocytin–streptavidin–Texas red conjugate. GAD was labelled using a primary antibody which detected both GAD-65 and GAD-67. Figure 6*C* is an overlay of the green coloured puncta from Fig. 6*A* onto the red

© 2009 The Authors. Journal compilation © 2009 The Physiological Society

coloured cell body from Fig. 6*B*. The appearance of yellow spots identifies the neuron as GABAergic by virtue of the colocalization of GAD immunoreactivity with the biocytin.

BDNF had no effects on the resting membrane potential, rheobase, excitability or input resistance of either GAD+ or GAD− neurons (Fig. 6*D* and *E* and Table 3). It did, however, decrease the frequency and amplitude of sEPSCs in GAD+ cells (Fig. 6*F* and *G*). These changes were significant according to both the Kolmogorov–Smirnov test (Fig. 6*F* and *G*) and comparison of mean amplitudes and IEI using a *t* test (Table 3). By contrast, the frequency of sEPSCs in GAD−, putative excitatory neurons was unchanged (Fig. 6*H*) but the amplitude was increased (Fig. 6*I*). The latter was significant according to the Kolmogorov–Smirnov test (Fig. 6*I*) but of marginal significance upon comparison with a *t* test (Table 3).

Does BDNF mediate the effects of CCI?

We have previously used confocal Fluo-4-AM imaging techniques to measure the Ca^{2+} response to high K^+ challenge in populations of dorsal horn neurons and have shown that BDNF increases the peak amplitude of such responses as might be expected if overall excitability is increased (Lu *et al.* 2007). This effect is illustrated in some typical recordings of Ca^{2+} responses in control and BDNF treated neurons (Fig. 7*A* and *B*). Five to six days' treatment with BDNF significantly increased both the peak amplitude (Fig. 7*C*) of the fluorescence response and the area under the curve (AUC, Fig. 7*D*).

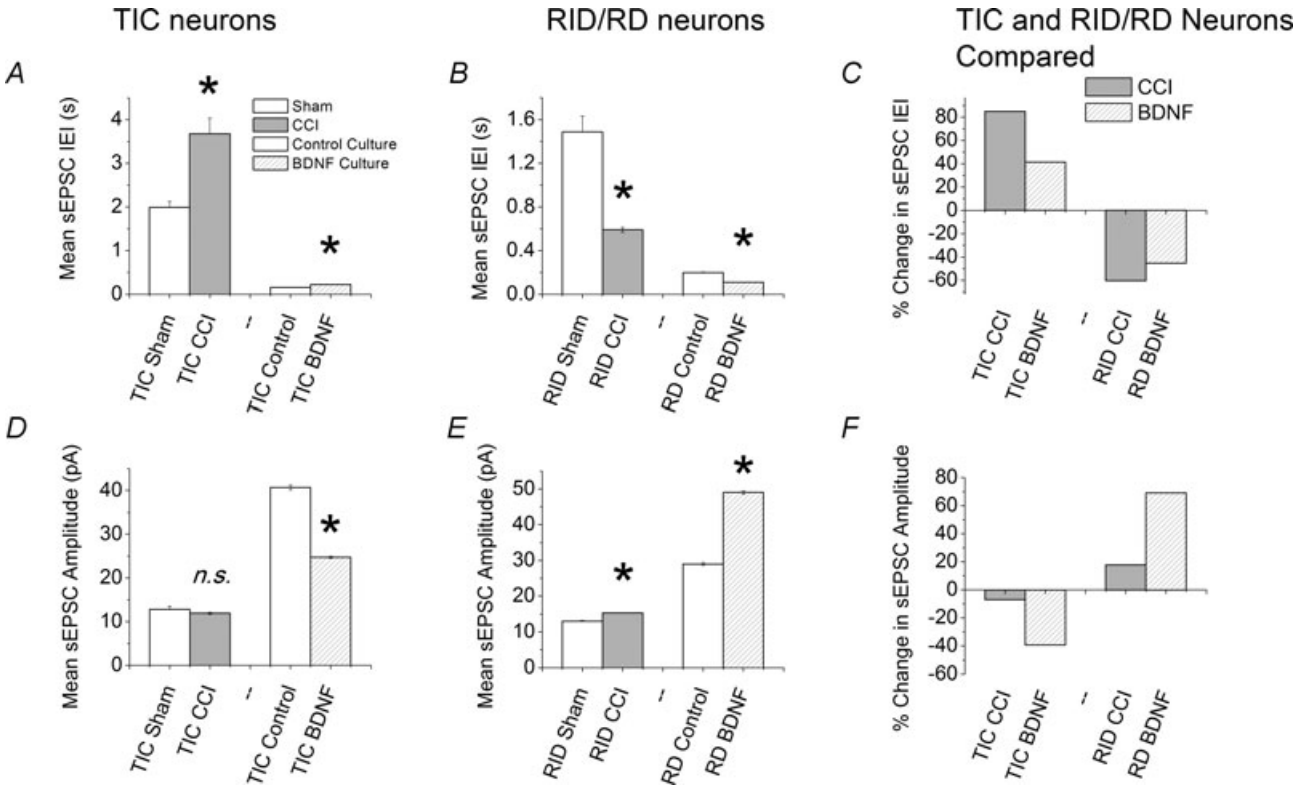

Figure 5. Bar graphs to illustrate similarity of effects of CCI and BDNF on excitatory transmission to TIC and to RID/RD neurons

Data were plotted from the same events lists used to produce Figs 2 and 4 panels *D*, *E*, *G* and *H*. $^*P < 0.001$ (Student's *t* test). In some cases, error bars are too small to be visible at this figure size (for numerical values see Tables 1 and 2). *A*, comparison of mean IEI for sEPSCs in TIC neurons in slices from sham and CCI animals as well as those in control or BDNF treated cultures. *B*, comparison of mean IEI in sham and CCI RID neurons in acute slices and control and BDNF-treated RD neurons in organotpic slice culture. *C*, comparison of percentage changes in IEI calculated (without error bars) from data in *A* and *B*. Note that both BDNF and CCI produce the same types of changes in IEI in both TIC and RID/RD neurons. *D*, comparison of sEPSC amplitude for TIC neurons in slices from sham and CCI animals and in control or BDNF-treated cultures. *E*, comparison of mean sEPSC amplitude in sham, CCI, control and BDNF-treated RID/RD neurons. *F*, comparison of percentage changes in sEPSC amplitude calculated (without error bars) from data in *D* and *E*. Note that both BDNF and CCI produce the same types of changes in sEPSC amplitude in both TIC and RID/RD neurons. Key in *A* applies also to *B*, *D* and *E*. Key in *C* also applies to *F*.

© 2009 The Authors. Journal compilation © 2009 The Physiological Society

To mimic the *in vivo* effect of CCI in the *in vitro* situation, we took advantage of the observation that activation of spinal microglia is one of the early consequences of peripheral nerve injury (Moss *et al.* 2007; Tsuda *et al.* 2005) and exposed organotypic cultures to medium that had been conditioned by exposure to activated microglia (aMCM). Figure 7*E* shows that the area under the curve and peak amplitude of K^+-induced Ca^{2+} responses were increased when cultures were exposed to aMCM for 5–6 days. This effect was not seen in organotypic cultures exposed to control medium from resting microglia (Fig. 7*F*).

If BDNF is responsible for the increased excitability seen with aMCM, its effect should be prevented by inclusion of the recombinant protein TrkB-d5, which binds and inactivates all neurotrophins that interact with TrkB receptors (Banfield *et al.* 2001). These experiments were done in two ways, TrkB-d5 was either included in the aMCM prior to introducing it into the organotypic cultures (Fig. 7*G*) or was added to the organotypic cultures prior to exposure to aMCM (Fig. 7*H*). In both cases, the effect of aMCM was abrogated by TrkBd5 (Fig. 7*F–J*). These results suggest that BDNF is a likely mediator of the excitatory actions of aMCM. Since microglial activation is

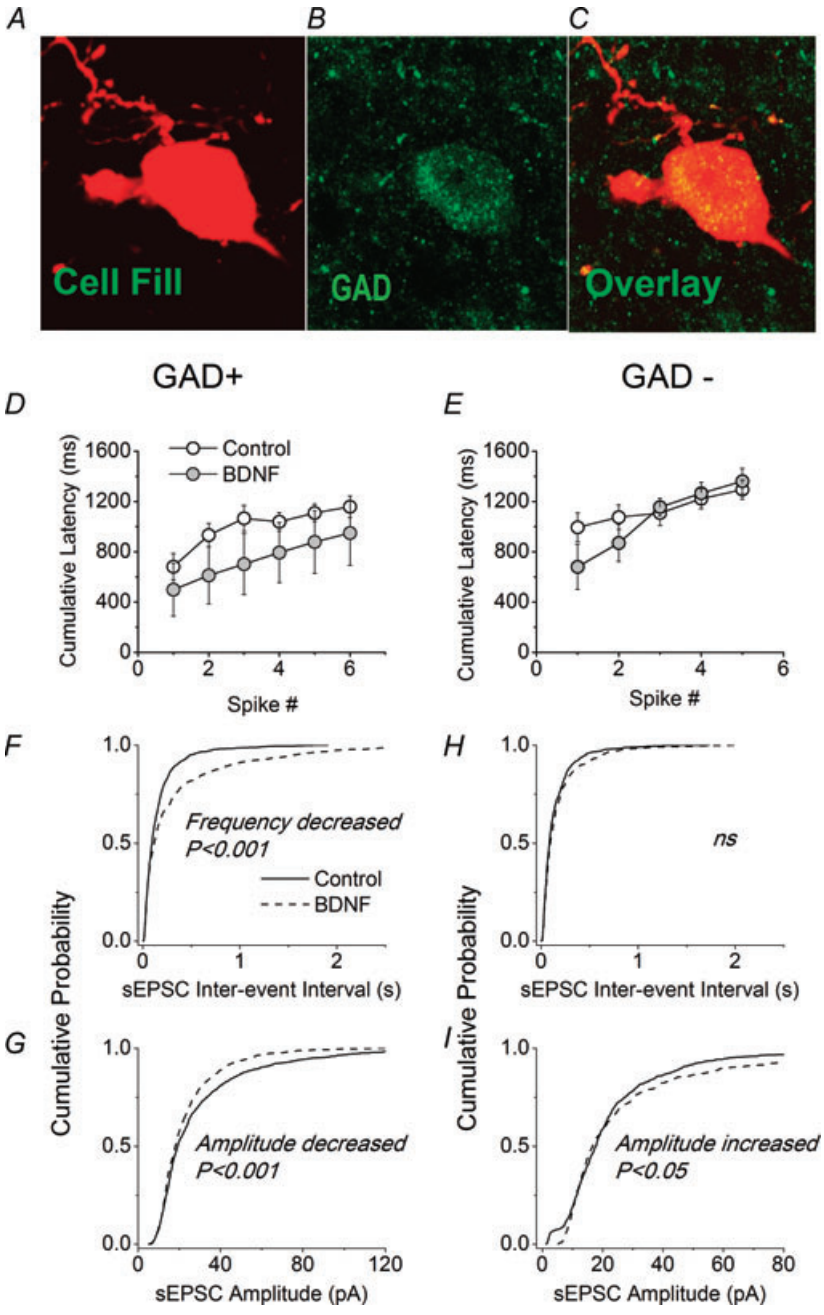

Figure 6. Effects of BDNF on GAD+ and GAD− neurons in organotypic slices
A, biocytin/Texas red fill of a neuron in the superficial dorsal horn of an organotypic slice. *B*, same field of view stained for glutamic acid decarboxylase (GAD) (both 65 and 67 kDa isoforms). *C*, overlay of *A* and *B* to show colocalization of GAD in the recorded neurons. *D* and *E*, lack of effect of BDNF on excitability of GAD+ and GAD− cells, respectively. Excitability was assessed by measuring the cumulative latency to the first and subsequent spikes in response to a depolarizing current ramp of 67 pA s^{-1}. Data obtained from control neurons (○) were not statistically different from those obtained from neurons exposed to BDNF (grey circles). Control data from 8 GAD+ neurons and 7 GAD− neurons; BDNF data from 3 GAD+ neurons and 3 GAD- neurons. *F–I*, cumulative probability plots for effects of BDNF on IEI and amplitude of sEPSCs in GAD+ and GAD− neurons. Data for all plots were obtained from the first 100 events following the first minute of recording from 11 GAD+ and 8 GAD− control neurons and 11 GAD+ and 7 GAD− neurons exposed to BDNF.

© 2009 The Authors. Journal compilation © 2009 The Physiological Society

Table 3 Effect of BDNF on electrophysiological properties of GAD+ and GAD− neurons

	GAD+ neurons	GAD− neurons
RMP control (mV)	−51.9 ± 3.1 ($n = 10$)	−49.1 ± 3.9 ($n = 8$)
RMP BDNF (mV)	−49.1 ± 2.3 ($n = 11$; $P > 0.4$)	−54.7 ± 2.2 ($n = 7$; $P > 0.2$)
Rheobase control (pA)	59.2 ± 9.9 ($n = 12$)	65.0 ± 11.6 ($n = 9$)
Rheobase BDNF (pA)	106.8 ± 21.6 ($n = 11$; $P > 0.05$)	82.9 ± 18.6 ($n = 7$; $P > 0.4$)I
Input Resistance control (MΩ)	246 ± 39 ($n = 11$)	437 ± 90 ($n = 9$)
Input Resistance BDNF (MΩ)	317 ± 48 ($n = 11$; $P > 0.15$)	265 ± 63 ($n = 7$; $P > 0.15$)
sEPSC		
IEI control (ms)	159.2 ± 6.3 ($n = 1100$ events from 11 neurons)	751.6 ± 32.3 ($n = 1017$ events from 8 neurons)
IEI BDNF (ms)	338.7 ± 17.8 ($n = 1100$ events from 11 neurons; $P = 0.05$)	661.3 ± 33.7 ($n = 829$ events from 7 neurons; $P < 0.0001$)
Amplitude control (pA)	28.9 ± 0.77 ($n = 1100$ events from 11 neurons)	24.4 ± 1.1 ($n = 800$ events from 8 neurons)
Amplitude BDNF (pA)	23.0 ± 0.47 ($n = 1100$ events from 11 neurons; $P = 0.05$)	27.5 ± 1.1 ($n = 700$ events from 7 neurons; $P < 0.0001$)

Data expressed as means ± S.E.M. *P*-values refer to comparison of data from control and BDNF treated groups. RMP, resting membrane potential; IEI, interevent interval. sEPSC statistics obtained from all events occurring within a 3 min recording period.

one of the early consequences of CCI (Tsuda *et al.* 2005; Coull *et al.* 2005; Moss *et al.* 2007), BDNF may mediate the overall increase in dorsal horn activity associated with central sensitization.

The electrophysiological experiments described above deal entirely with changes in excitatory transmission yet it is well recognized that changes in inhibitory synaptic transmission contribute both to central sensitization and to the effect of BDNF (Coull *et al.* 2003, 2005; Price *et al.* 2005). It is possible therefore that the overall increase in excitability seen with BDNF and aMCM are primarily attributable to attenuation of inhibition. To test this possibility, we examined the effect of BDNF in organotypic slice cultures where GABAergic transmission was blocked with the selective $GABA_A$ antagonist SR95531. Figure 8*A* illustrates the increase in peak amplitude of the Ca^{2+} response seen when BDNF treated cultures were challenged with 35 mM K^+. Figure 8*B* shows that this increase persists in the presence of 10 μM SR95531. Similarly, for the area under the curve (AUC), the increase produced by BDNF (Fig. 8*C*) persisted in the presence of SR95531 (Fig. 8*D*). Corresponding sample recordings are shown in Fig. 8*E–H*. Blockade of $GABA_A$ receptors with SR95531 appeared to increase the duration of Ca^{2+} responses to 35 mM K^+ in both control (Fig. 8*G* compared to Fig. 8*E*) and BDNF treated cultures (Fig. 8*H* compared to Fig. 8*F*). The antagonist also enhanced or initiated large oscillations in baseline Ca^{2+} levels (Fig. 8*J* compared to Fig. 8*I*). The latter two observations serve as positive controls for the effectiveness of SR95531. Thus, BDNF is still capable of increasing excitability when $GABA_A$ receptors are blocked; this is consistent with a BDNF-induced change in excitatory synaptic transmission.

If this is the case, the K^+ evoked Ca^{2+} response should be mediated, at least in part, by the depolarization induced release of glutamate. To test this, we examined the effect of the glutamate uptake blocker dihydrokainate (DHK 0.1 mM; Arriza *et al.* 1994) on Ca^{2+} signals generated by exposure to 35 mM K^+. In control neurons, DHK slowed the rate of decay of the Ca^{2+} signal. Time for 20% recovery (t_{20}) was increased from 61.8 ± 4.1 s to 93.1 ± 4.1 s ($n = 19$, $P < 0.02$, paired t test). A typical experiment is illustrated in Fig. 8*K*.

Effects of a mixture of iontotropic glutamate receptor antagonists (1 μM CNQX plus 10 μM AP-5) were more complex. Although the antagonist mixture had little effect on Ca^{2+} responses to 35 mM K^+ in control cultures, it had a clear effect on those treated with BDNF. The drugs reduced the peak amplitude of the Ca^{2+} response by 36.6%

© 2009 The Authors. Journal compilation © 2009 The Physiological Society

from 800 ± 215 to 509 ± 145 arbitrary fluorescence units ($n = 9$, $P < 0.005$, paired t test). There was also a very clear increase in the latency of the onset of the Ca^{2+} signal, which increased from 118 ± 2.7 to 173 ± 8.8 s ($n = 9$ $P < 0.0002$, paired t test). A typical experiment is illustrated in Fig. 8*L*.

These findings are consistent with the involvement of depolarization-induced glutamate release in the Ca^{2+} response to K^+ challenge.

Discussion

The main findings of this study are that (1) CCI increases excitatory synaptic drive to putative excitatory neurons in the rat substantia gelatinosa and decreases that to putative inhibitory neurons, (2) a very similar pattern of changes is produced by BDNF, and (3) there may be a cause and effect relationship between these two phenomena.

Neuronal phenotypes in acute slices of substantia gelatinosa and effects of CCI

One of the difficulties associated with studying substantia gelatinosa is that there is no universally accepted definition of the neuronal phenotypes found therein. Neurons have been classified in terms of morphological (Todd & Lewis, 1986; Todd & Spike, 1993; Bailey

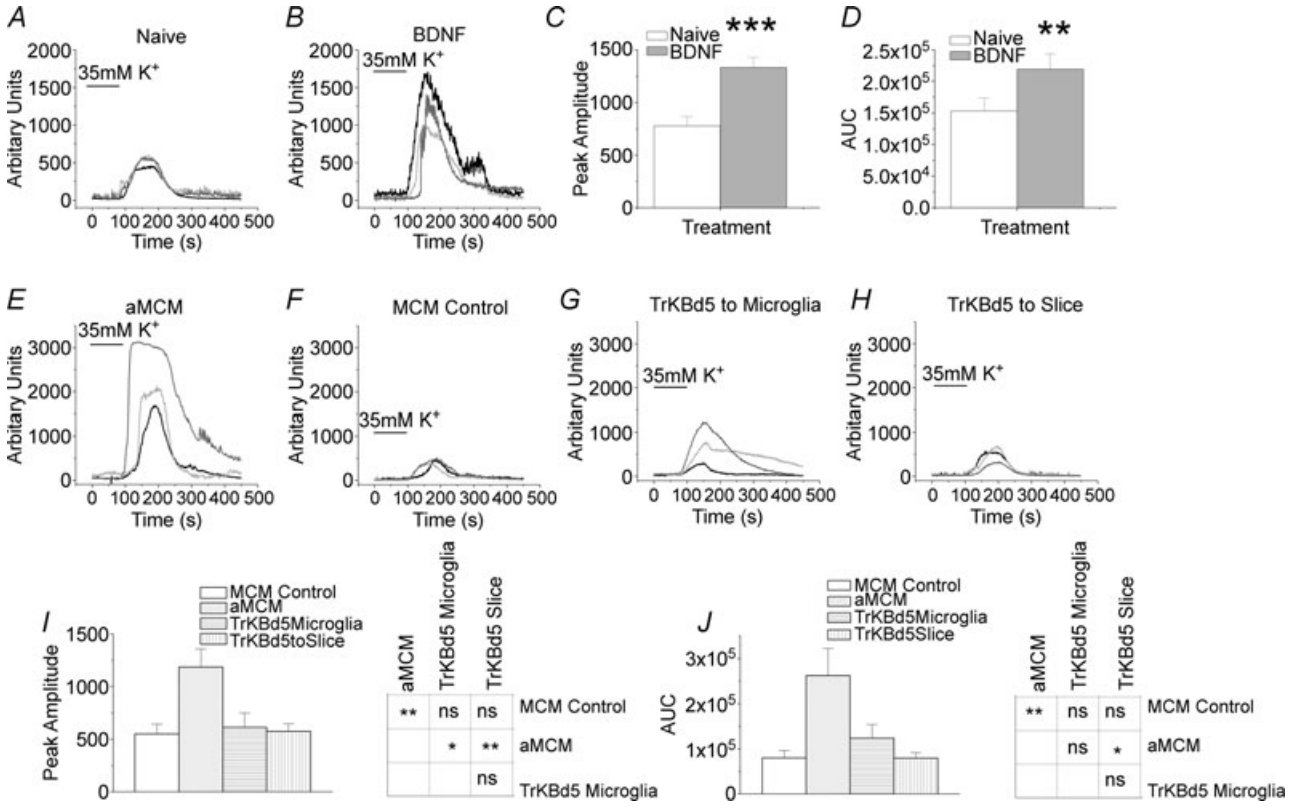

Figure 7. Population excitability of dorsal horn cells as measured by real-time changes in $[Ca^{2+}]_i$-dependent Fluo-4-AM fluorescence in response to 35 mM K^+

A, lines illustrate responses of three control neurons in naive (untreated) organonotypic slice culture. *B*, responses of three different neurons from a BDNF-treated culture. *C* and *D*, comparison of amplitude and area under the fluorescence signal traces (AUC) in control and BDNF-treated culture slices ($n = 38$ cells for control, $n = 25$ cells for BDNF). Both amplitude and area of the Ca^{2+} signal were significantly larger in BDNF-treated cells (t test; $^{**}P < 0.001$, $^{*}P < 0.05$). Amplitude scaling is in arbitrary units, AUC scaling is in arbitrary amplitude units × time (s). *E*, responses of three neurons in culture exposed to activated microglia-conditioned medium (aMCM). *F*, responses of three neurons in culture exposed to unactivated microglia-conditioned media (MCM control). *G*, responses of three neurons exposed to aMCM that had been preincubated with 7.5 μM TrkB-d5 to bind any BDNF in the medium. The TrkB-d5 was added to the microglia cultures immediately after LPS stimulation. *H*, responses of three neurons to aMCM after preincubation of slices with 7.5 μM TrkB-d5. *I*, comparison of amplitude of K^+-induced fluorescence signals in MCM control, aMCM-treated slices, aMCM-treated slices pre-incubated with TrkB-d5 added to the microglia and aMCM-treated slices preincubated with TrkB-d5. *J*, comparison of AUC of the Ca^{2+} fluorescence signal traces in MCM control, aMCM-treated slices and aMCM-treated slices preincubated with TrkB-d5 added either to the microglia or to the slice. For *I* and *J*, $n = 22$ cells for MCM control, $n = 28$ cells for aMCM and $n = 19$ for aMCM plus TrkB-d5 to microglia and $n = 28$ cells for MCM plus TrkB-d5 to slice. One way ANOVA with Tukey–Kramer *post hoc* tests; $^{**}P < 0.001$, $^{*}P < 0.05$. Error bars indicate S.E.M. Note that the bar labelled K^+ indicates time of change of superfusate in the reservoir bottles and not in the recording chamber.

© 2009 The Authors. Journal compilation © 2009 The Physiological Society

& Ribeiro-da-Silva, 2006), electrophysiological (Ruscheweyh & Sandkuhler, 2002; Grudt & Perl, 2002; Lu & Perl, 2003, 2005; Balasubramanyan *et al.* 2006; Santos *et al.* 2007) and immunohistochemical/transmitter phenotype criteria (Heinke *et al.* 2004; Schoffnegger *et al.* 2006) and there is still debate as to whether certain morphologies always associate with specific neurotransmitter phenotypes and/or electrophysiological

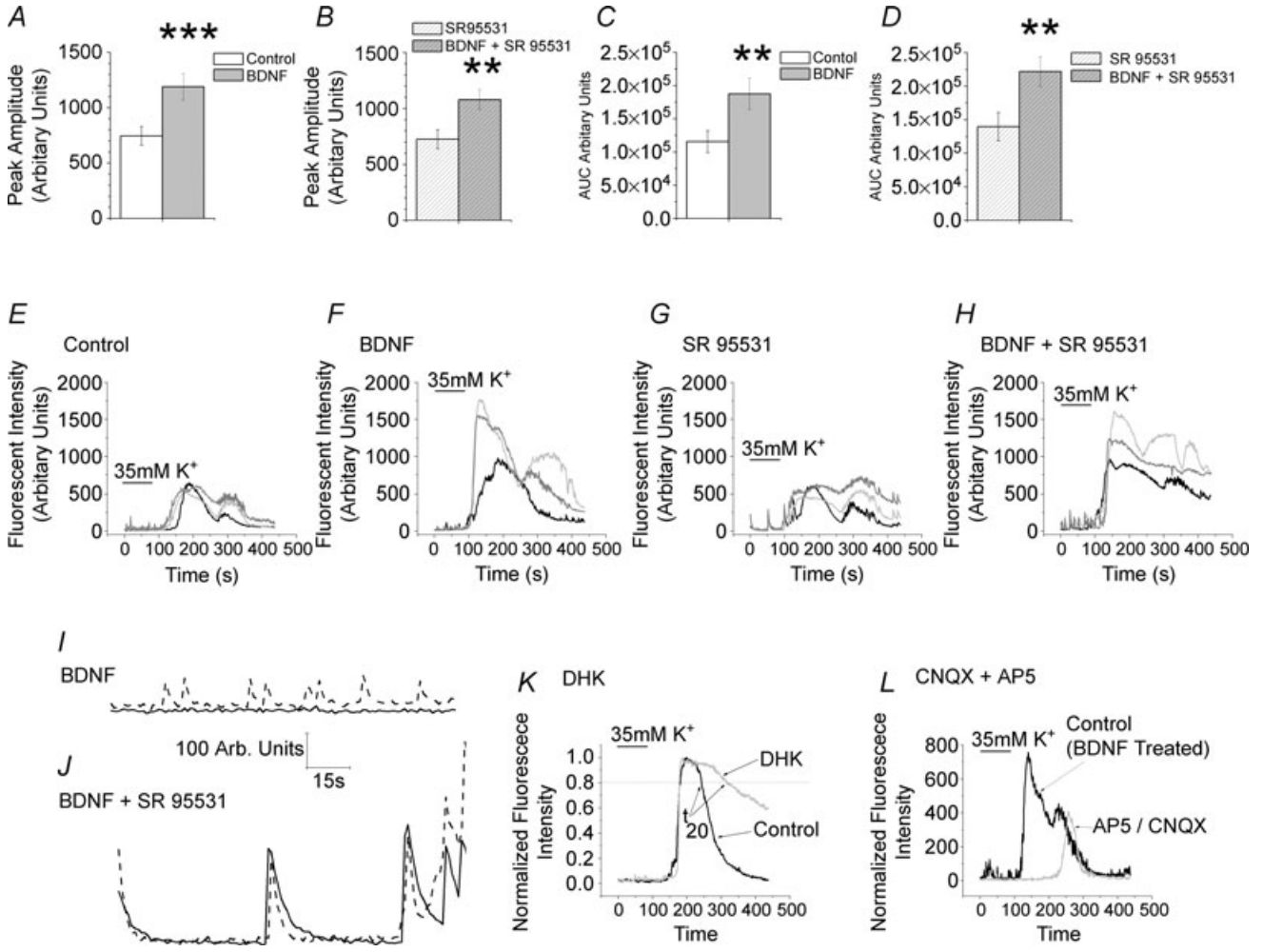

Figure 8. Effects of blockade of $GABA_A$ or iontropic glutamate receptors and blockade of EAAT2 on BDNF induced changes in population excitability of dorsal horn neurons

A, difference in peak amplitude of cytosolic Ca^{2+} response to 35 mM K^+ between control neurons and those exposed to 200 ng ml^{-1} BDNF. *B*, persistence of difference in peak amplitude of responses to BDNF in neurons treated with 10 μM SR95531 for 15 min. *C*, difference in AUC of Ca^{2+} response to 35 mM K^+ following long-term exposure to 200 ng ml^{-1} BDNF. *D*, persistence in difference of AUC of responses to BDNF in neurons treated with 10 μM SR95531 for 15 min. Data from 18 control neurons that were subsequently exposed to SR95531 and from 18 neurons exposed to BDNF that were subsequently exposed to SR95531. Error bars indicate S.E.M., $^{**}P < 0.02$, $^{***}P < 0.005$. *E* and *H*, sample recordings of Ca^{2+} signals in control, BDNF treated, SR95531 and BDNF treated + SR95531 neurons in response to 35 mM K^+. Note longer durations of responses recorded in SR95531. *I* and *J*, sample records of baseline Ca^{2+} levels in two BDNF-treated control neurons before (*I*) and 15 min after start of superfusion with10 μM SR95531 (*J*). The antagonist appeared to increase the amplitude of oscillations in a cell that was already oscillating (dashed trace) and induced oscillations in a cell that previously exhibited a stable baseline Ca^{2+} level (continuous trace). *K*, effect of 0.1 mM dihydrokainate (DHK) on Ca^{2+} response to 35 mM K^+ challenge. Superimposed recordings of control response and that seen in DHK in the same neuron. Note slowing of rate of decay. Arrows designate points for measuring t_{20} values, i.e. the times to 20% recovery of the Ca^{2+} response. *L*, effects of a combination of AP-5 (10 μM) and CNQX (1 μM) on Ca^{2+} responses to 35 mM K^+. Superimposed recordings from the same neuron prior to and after glutamate blockade. Culture had been exposed to BDNF for 6 days prior to study. Note profound increase in response latency seen in the presence of CNQX/AP-5 and decreased response amplitude. Note that bar labelled K^+ indicates time of change of superfusate in the reservoir bottles and not in the recording chamber.

© 2009 The Authors. Journal compilation © 2009 The Physiological Society

properties. Data presented in Fig. 1*J* contribute to this debate as they underline some of the generalizations that can be made. For example, although there is good correlation between islet/central cell morphology and tonic firing, quite a few islet/central cells display the phasic firing pattern. Whilst some phasic cells are likely to be GABAergic (Heinke *et al.* 2004; Schoffnegger *et al.* 2006), others may be excitatory (Lu & Perl, 2005). For the purposes of comparison of neurons from CCI and sham operated animals, we therefore selected a restricted population of neurons (tonic, islet/central TIC cells) as both their morphology and firing properties have been associated with inhibitory substantia gelatinosa neurons (Lu & Perl, 2003; Todd & Spike, 1993). Thus, the decrease in sEPSC frequency seen in TIC cells (Fig. 2*D*) suggests that CCI reduces excitatory synaptic drive to at least one major population of inhibitory neurons. Additional evidence to support this idea comes from ultrastructural studies that show that CCI promotes transient loss of the excitatory synaptic terminals of non-peptidergic nociceptive fibres in substantia gelatinosa (Bailey & Ribeiro-da-Silva, 2006). This is relevant because these fibres form the synaptic terminals of the type 1 synaptic glomeruli (Ribeiro & Coimbra, 1982) that associate with GABAergic neurons (Todd, 1996). Because nerve injury does not promote loss of GABA immunoreactivity or alteration in $GABA_A$ receptors, decreased firing of inhibitory neurons was recently proposed to play a role in the onset of allodynia (Polgar & Todd, 2008).

We also studied RID (radial irregular delay) neurons in acute slices as a delayed firing pattern has been associated with excitatory neurons. For example, in paired recordings in substantia gelatinosa, intracellular stimulation of delay firing cells produced excitatory events in postsynaptic neurons (Lu & Perl, 2005). Other studies using a transgenic mouse strain coexpressing enhanced green fluorescent protein under the control of the GAD-67 promotor associated the GABA phenotype with initial burst (phasic), gap (irregular) or tonic and not with delay firing patterns (Schoffnegger *et al.* 2006). We therefore suggest that RID neurons are predominantly excitatory and the CCI-induced increase in sEPSC frequency (Fig. 2*G*) and amplitude (Fig. 2*H*) in this population reflects increased synaptic drive to excitatory neurons.

Neuronal phenotypes in organotypic slices

Similarities between firing patterns and associated morphologies of neurons in acute slices (Fig. 1*J*) to those in organotypic culture (Fig. 3*I*) add support to the notion that the cultures bear considerable developmental similarity to acute slices (Avossa *et al.* 2003; Lu *et al.* 2006) For example, islet cells frequently display a tonic firing pattern both in acute slices (Fig. 1*J*) and in organotypic cultures (Fig. 3*I*) and delay cells associate with vertical or radial morphologies in both situations.

We suggest that the slight difference in firing pattern of radial neurons in culture (RD cells) and radial neurons in acute slices (RID) may reflect the finding that the cell bodies of some substantia gelatinosa neurons in acute slices do not generate action potentials (Safronov *et al.* 1999), so the typically low amplitude of action potentials seen in RID cells may reflect passive invasion of the soma from the axons. By contrast, we have previously noted that neurons in organotypic slice cultures are generally more excitable than neurons in acute slices (Lu *et al.* 2006) and this may enable the more stable discharge of large somatic action potentials in radial neurons in culture.

Similarity of action of BDNF and CCI

Under the conditions of our whole-cell recording experiments, neither CCI nor BDNF appear to affect passive neuronal properties or indices of membrane excitability (Fig. 2*A* and *B*, Fig. 4*A* and *B*, Tables 1–3). Changes are instead confined to alterations in excitatory synaptic transmission and for most aspects studied there is a good correspondence between the actions of CCI and those of BDNF in TIC and RID/RD neurons (Fig. 5). There are, however, some small differences. For example, CCI does not affect sEPSC amplitude in TIC cells (Figs 2*E* and 5*D*) whereas BDNF reduces it (Figs 4*E* and 5*A*). One possible explanation for this discrepancy is that slightly different populations of neurons may have been sampled in organotypic culture slices compared to acute slices. Whilst lamina II can be readily identified visually in acute slices, we sampled neurons from an area 0.5–2 mm from the dorsal surface of the cultures. Because phasic, delay and tonic firing neurons can be found in both lamina I (Prescott & de Koninck, 2002) and in laminae III/IV (Schneider, 2008), it is possible that some of neurons sampled in our organotypic cultures came from these regions. Moreover, these cells may respond differently to BDNF from those in lamina II. Although this possibility cannot be discounted, there are no instances where the effects of BDNF in organotypic culture were the opposite of those of CCI in acute slices (Fig. 5*C* and *F*). We therefore suggest that the minor differences in their actions are quantitative rather than qualitative. Two additional arguments support our contention that BDNF and CCI initiate similar processes. First, we have shown that the effects of BDNF on the whole population of tonic firing neurons involve an increase in the rate of decay of miniature EPSCs (mEPSCs) (Lu *et al.* 2007) and a similar change is seen in this cell type with CCI (S. Balasubramanyan & P. A. Smith, unpublished observations). Both may reflect an increased contribution of Ca^{2+} permeable AMPA channels to synaptic currents (Vikman *et al.* 2007). Second, both BDNF (Lu *et al.* 2007) and CCI (S. Balasubramanyan & P. A. Smith,

© 2009 The Authors. Journal compilation © 2009 The Physiological Society

unpublished observations) promote the appearance of a new population of large mEPSCs in the whole population of delay neurons.

Cellular mechanisms of BDNF action

Although the purpose of the present work is to explore the identity of action of CCI and BDNF and to seek to identify any cause and effect relationship between them, we have preliminary data regarding the action of BDNF on mEPSCs in TIC and RD neurons (V. B. Lu & P. A. Smith, unpublished observations). Analysis of mEPSC rather than sEPSCs allows more precise differentiation between a pre- or postsynaptic site of action. Thus, in TIC neurons, mEPSC amplitude is decreased whereas in RD neurons, mEPSC amplitude is increased. Changes in frequency are not significant but this may reflect the large standard error in the small populations of neurons so far tested (100 events in each of 3 neurons tested as TIC controls, TIC BDNF, RD controls or RD BDNF). These changes resemble those seen in our previous study where neurons were identified on the basis of purely electrophysiological criteria (Lu *et al.* 2007). Thus, BDNF reduced the amplitude and frequency of mEPSCs in tonic neurons but had the reverse effect in delay neurons; mEPSC amplitude and frequency were increased. Further statistical analysis of the behaviour of subpopulations of mEPSCs led us to suggest that actions of BDNF on synaptic transmission in delay neurons were exclusively presynaptic. By contrast, its actions on tonic neurons involved both and pre- and postsynaptic components. We think it likely therefore that actions of BDNF on TIC cells may involve the pre- and postsynaptic actions previously identified in tonic neurons while its actions on RD neurons, like those on the whole population of delay neurons may be exclusively presynaptic.

In view of this, it is pertinent to ask how BDNF exerts differential and sometimes opposing effects on different types of neuron. One possibility is that some effects are mediated by TrkB (Kaplan & Stephens, 1994) whereas others are mediated via the p75 neurotrophin receptor (Boyd & Gordon, 2001) and these receptors are expressed to different extents on various types of presynaptic terminals and cell bodies.

Role of BDNF in the effect of CCI and central sensitization

The observation that BDNF increases the Ca^{2+} response to a 35 mM K^+ challenge shows that long-term neurotrophin exposure increases overall dorsal horn excitability. That this increase in response reflects changes in glutamatergic transmission is supported by the observed effects of DHK. This substance has high affinity for the glial glutamate transporter EAAT2 (Arriza *et al.* 1994). The slowing of the recovery of the Ca^{2+} response presumably reflects the continued presence of released glutamate when its uptake via EAAT2 is compromised.

We do not know why the CNQX/AP-5 mixture is only effective in attenuating Ca^{2+} responses in BDNF treated cultures. The effectiveness of DHK on control cultures suggests that K^+ is clearly releasing glutamate under these conditions. One possibility is that part of the Ca^{2+} response reflects activation of metabotropic glutamate receptors. This possibility remains to be investigated. The increased latency of the Ca^{2+} response in the presence of CNQX/AP-5 is an interesting phenomenon which may reflect the slow increase in extracellular K^+ concentration following switching the superfusion to a reservoir containing 35 mM K^+. As K^+ concentration in the slice progressively increases, spontaneous transmitter release may be affected before membrane potential so that the earliest phase of the response is most susceptible to the action of glutamate antagonists.

The fact that the effect of BDNF on the K^+ induced Ca^{2+} response is mimicked by aMCM and the effect of aMCM is abrogated by TrkBd5 shows that activated microglia may be a source of BDNF. Since spinal microglia are activated by CCI (Coull *et al.* 2005) and BDNF and CCI produce a similar pattern of changes in TIC and RID/RD cells, it is likely that the effects of CCI are mediated by BDNF. Although TrkBd5 has affinity for neurotrophin-4 (Banfield *et al.* 2001), this substance is undetectable in both the intact and deafferented spinal cord (Ramer *et al.* 2007). Neurotrophin-4 is therefore unlikely to contribute to the effect of CCI.

Micoglial-derived BDNF has also been shown to mediate CCI-induced increases in spinal cord excitability by perturbation of the transmembrane Cl^- gradient and attenuation of the action of GABA on lamina I neurons (Coull *et al.* 2005; Prescott *et al.* 2006). It is possible therefore that the overall increase in excitability we observe is entirely attributable to altered GABAergic inhibition and the effects we have observed on excitatory synaptic transmission have little bearing on the overall increase in dorsal horn excitability. This does not appear to be the case as BDNF was still able to increase overall excitability in the presence of the $GABA_A$ antagonist SR95531. Nevertheless, these findings alone are not sufficient to exclude the important and well-documented contribution of alterations in Cl^- gradient to pain centralization (Coull *et al.* 2005). On the contrary, it is likely that altered GABAergic inhibition conspires with changes in excitatory transmission to produce altered nociceptive processing. It may therefore be suggested that BDNF is 'necessary and sufficient' to program many, if not all, of the changes that underlie CCI-induced changes in the superficial dorsal horn and which contribute to 'central sensitization'.

© 2009 The Authors. Journal compilation © 2009 The Physiological Society

References

Arriza JL, Fairman WA, Wadiche JI, Murdoch GH, Kavanaugh MP & Amara SG (1994). Functional comparisons of three glutamate transporter subtypes cloned from human motor cortex. *J Neurosci* **14**, 5559–5569.

Avossa D, Rosato-Siri MD, Mazzarol F & Ballerini L (2003). Spinal circuits formation: a study of developmentally regulated markers in organotypic cultures of embryonic mouse spinal cord. *Neuroscience* **122**, 391–405.

Bailey AL & Ribeiro-da-Silva A (2006). Transient loss of terminals from non-peptidergic nociceptive fibers in the substantia gelatinosa of spinal cord following chronic constriction injury of the sciatic nerve. *Neuroscience* **138**, 675–690.

Balasubramanyan S, Stemkowski PL, Stebbing MJ & Smith PA (2006). Sciatic chronic constriction injury produces cell-type specific changes in the electrophysiological properties of rat substantia gelatinosa neurons. *J Neurophysiol* **96**, 579–590.

Banfield MJ, Naylor RL, Robertson AG, Allen SJ, Dawbarn D & Brady RL (2001). Specificity in Trk receptor: neurotrophin interactions: the crystal structure of TrkB-d5 in complex with neurotrophin-4/5. *Structure* **9**, 1191–1199.

Boyd JG & Gordon T (2001). The neurotrophin receptors, trkB and p75, differentially regulate motor axonal regeneration. *J Neurobiol* **49**, 314–325.

Cho HJ, Kim JK, Park HC, Kim JK, Kim DS, Ha SO & Hong HS (1998). Changes in brain-derived neurotrophic factor immunoreactivity in rat dorsal root ganglia, spinal cord, and gracile nuclei following cut or crush injuries. *Exp Neurol* **154**, 224–230.

Coull JA, Beggs S, Boudreau D, Boivin D, Tsuda M, Inoue K, Gravel C, Salter MW & de Koninck Y (2005). BDNF from microglia causes the shift in neuronal anion gradient underlying neuropathic pain. *Nature* **438**, 1017–1021.

Coull JA, Boudreau D, Bachand K, Prescott SA, Nault F, Sik A, De Koninck P & De Koninck Y (2003). Trans-synaptic shift in anion gradient in spinal lamina I neurons as a mechanism of neuropathic pain. *Nature* **424**, 938–942.

Dalal A, Tata M, Allègre G, Gekiere F, Bons N & Albe-Fessard D (1999). Spontaneous activity of rat dorsal horn cells in spinal segments of sciatic projection following transection of sciatic nerve or of corresponding dorsal roots. *Neuroscience* **94**, 217–228.

Dougherty KD, Dreyfus CF & Black IB (2000). Brain-derived neurotrophic factor in astrocytes, oligodendrocytes, and microglia/macrophages after spinal cord injury. *Neurobiol Dis* **7**, 574–585.

Dougherty KJ, Sawchuk MA & Hochman S (2005). Properties of mouse spinal lamina I GABAergic interneurons. *J Neurophysiol* **94**, 3221–3227.

Garraway SM, Petruska JC & Mendell LM (2003). BDNF sensitizes the response of lamina II neurons to high threshold primary afferent inputs. *Eur J Neurosci* **18**, 2467–2476.

Gobel S (1978). Golgi studies of the neurons in layer II of the dorsal horn of the medulla (trigeminal nucleus caudalis). *J Comp Neurol* **180**, 395–414.

Graham BA, Brichta AM & Callister RJ (2007). Moving from an averaged to specific view of spinal cord pain processing circuits. *J Neurophysiol* **98**, 1057–1063.

Groth R & Aanonsen L (2002). Spinal brain-derived neurotrophic factor (BDNF) produces hyperalgesia in normal mice while antisense directed against either BDNF or trkB, prevent inflammation-induced hyperalgesia. *Pain* **100**, 171–181.

Grudt TJ & Perl ER (2002). Correlations between neuronal morphology and electrophysiological features in the rodent superficial dorsal horn. *J Physiol* **540**, 189–207.

Heinke B, Ruscheweyh R, Forsthuber L, Wunderbaldinger G & Sandkuhler J (2004). Physiological, neurochemical and morphological properties of a subgroup of GABAergic spinal lamina II neurones identified by expression of green fluorescent protein in mice. *J Physiol* **560**, 249–266.

Iadarola MJ & Caudle RM (1997). Good pain, bad pain. *Science* **278**, 239–240.

Kaplan DR & Stephens RM (1994). Neurotrophin signal transduction by the Trk receptor. *J Neurobiol* **25**, 1404–1407.

Kim KJ, Yoon YW & Chung JM (1997). Comparison of three rodent models of neropahic pain. *Exp Brain Res* **113**, 200–206.

Lu VB, Ballanyi K, Colmers WF & Smith PA (2007). Neuron type-specific effects of brain-derived neurotrophic factor in rat superficial dorsal horn and their relevance to 'central sensitization'. *J Physiol* **584**, 543–563.

Lu VB, Moran TD, Balasubramanyan S, Alier KA, Dryden WF, Colmers WF & Smith PA (2006). Substantia gelatinosa neurons in defined-medium organotypic slice culture are similar to those in acute slices from young adult rats. *Pain* **121**, 261–275.

Lu Y & Perl ER (2003). A specific inhibitory pathway between substantia gelatinosa neurons receiving direct C-fiber input. *J Neurosci* **23**, 8752–8758.

Lu Y & Perl ER (2005). Modular organization of excitatory circuits between neurons of the spinal superficial dorsal horn (laminae I and II). *J Neurosci* **25**, 3900–3907.

Maxwell DJ, Belle MD, Cheunsuang O, Stewart A & Morris R (2007). Morphology of inhibitory and excitatory interneurons in superficial laminae of the rat dorsal horn. *J Physiol* **584**, 521–533.

Moore KA, Kohno T, Karchewski LA, Scholz J, Baba H & Woolf CJ (2002). Partial peripheral nerve injury promotes a selective loss of GABAergic inhibition in the superficial dorsal horn of the spinal cord. *J Neurosci* **22**, 6724–6731.

Moran TD, Colmers WF & Smith PA (2004). Opioid-like actions of neuropeptide Y in rat substantia gelatinosa: Y1 suppression of inhibition and Y2 suppression of excitation. *J Neurophysiol* **92**, 3266–3275.

Mosconi T & Kruger L (1996). Fixed-diameter polyethylene cuffs applied to the rat sciatic nerve induce a painful neuropathy: ultrastructural morphometric analysis of axonal alterations. *Pain* **64**, 37–57.

Moss A, Beggs S, Vega-Avelaira D, Costigan M, Hathway GJ, Salter MW & Fitzgerald M (2007). Spinal microglia and neuropathic pain in young rats. *Pain* **128**, 215–224.

Polgar E & Todd AJ (2008). Tactile allodynia can occur in the spared nerve injury model in the rat without selective loss of GABA or $GABA_A$ receptors from synapses in laminae I–II of the ipsilateral spinal dorsal horn. *Neuroscience* **156**, 193–202.

© 2009 The Authors. Journal compilation © 2009 The Physiological Society

Prescott SA & de Koninck Y (2002). Four cell types with distinctive membrane properties and morphologies in lamina I of the spinal dorsal horn of the adult rat. *J Physiol* **539**, 817–836.

Prescott SA, Sejnowski TJ & de Koninck Y (2006). Reduction of anion reversal potential subverts the inhibitory control of firing rate in spinal lamina I neurons: towards a biophysical basis for neuropathic pain. *Mol Pain* **2**, 32.

Price TJ, Cervero F & de Koninck Y (2005). Role of cation-chloride-cotransporters (CCC) in pain and hyperalgesia. *Curr Top Med Chem* **5**, 547–555.

Ramer LM, McPhail LT, Borisoff JF, Soril LJ, Kaan TK, Lee JH, Saunders JW, Hwi LP & Ramer MS (2007). Endogenous TrkB ligands suppress functional mechanosensory plasticity in the deafferented spinal cord. *J Neurosci* **27**, 5812–5822.

Ribeiro-da-Silva A & Coimbra A (1982). Two types of synaptic glomeruli and their distribution in laminae I–III of the rat spinal cord. *J Comp Neurol* **209**, 176–186.

Ruangkittisakul A, Schwarzacher SW, Secchia L, Poon BY, Ma Y, Funk GD & Ballanyi K (2006). High sensitivity to neuromodulator-activated signaling pathways at physiological $[K^+]$ of confocally imaged respiratory center neurons in on-line-calibrated newborn rat brainstem slices. *J Neurosci* **26**, 11870–11880.

Ruscheweyh R & Sandkuhler J (2002). Lamina-specific membrane and discharge properties of rat spinal dorsal horn neurons *in vitro*. *J Physiol* **541**, 231–244.

Safronov BV, Wolff M & Vogel W (1999). Axonal expression of sodium channels in rat spinal neurones during postnatal development. *J Physiol* **514**, 729–734.

Santos SF, Rebelo S, Derkach VA & Safronov BV (2007). Excitatory interneurons dominate sensory processing in the spinal substantia gelatinosa of rat. *J Physiol* **581**, 241–254.

Schneider SP (2008). Local circuit connections between hamster laminae III and IV dorsal horn neurons. *J Neurophysiol* **99**, 1306–1318.

Schoffnegger D, Heinke B, Sommer C & Sandkuhler J (2006). Physiological properties of spinal lamina II GABAergic neurons in mice following peripheral nerve injury. *J Physiol* **577**, 869–878.

Siao CJ & Tsirka SE (2002). Tissue plasminogen activator mediates microglial activation via its finger domain through annexin II. *J Neurosci* **22**, 3352–3358.

Thompson SW, Bennett DL, Kerr BJ, Bradbury EJ & McMahon SB (1999). Brain-derived neurotrophic factor is an endogenous modulator of nociceptive responses in the spinal cord. *Proc Natl Acad Sci U S A* **96**, 7714–7718.

Todd AJ (1996). GABA and glycine in synaptic glomeruli of the rat spinal dorsal horn. *Eur J Neurosci* **8**, 2492–2498.

Todd AJ & Lewis SG (1986). The morphology of Golgi-stained neurons in lamina II of the rat spinal cord. *J Anat* **149**, 113–119.

Todd AJ & Spike RC (1993). The localization of classical transmitters and neuropeptides within neurons in laminae I–III of the mammalian spinal dorsal horn. *Prog Neurobiol* **41**, 609–645.

Treede R-D, Jensen TS, Campbell JN, Cruccu G, Dostrovsky JO, Griffin JW, Hansson P, Hughes R, Nurmikko T & Serra J (2008). Neuropathic pain: Redefinition and a grading system for clinical and research purposes. *Neurology* **70**, 1630–1635.

Tsuda M, Inoue K & Salter MW (2005). Neuropathic pain and spinal microglia: a big problem from molecules in 'small' glia. *Trends Neurosci* **28**, 101–107.

Tsuda M, Shigemoto-Mogami Y, Koizumi S, Mizokoshi A, Kohsaka S, Salter MW & Inoue K (2003). P2X4 receptors induced in spinal microglia gate tactile allodynia after nerve injury. *Nature* **424**, 778–783.

Vikman KS, Rycroft BK & Christie MJ (2007). Switch to Ca^{2+} permeable AMPA and reduced NR2B NMDA receptor mediated neurotransmission at dorsal horn nociceptive synapses during inflammatory pain in the rat. *J Physiol* **586**, 515–527.

Woolf CJ (1983). Evidence for a central component of post-injury pain hypersensitivity. *Nature* **306**, 686–688.

Woolf CJ & Mannion RJ (1999). Neuropathic pain: aetiology, symptoms, mechanisms, and management. *Lancet* **353**, 1959–1964.

Yajima Y, Narita M, Usui A, Kaneko C, Miyatake M, Narita M, Yamaguchi T, Tamaki H, Wachi H, Seyama Y & Suzuki T (2005). Direct evidence for the involvement of brain-derived neurotrophic factor in the development of a neuropathic pain-like state in mice. *J Neurochem* **93**, 584–594.

Acknowledgements

Supported by grants from the Canadian Institutes of Health Research (CIHR), Christopher Reeve Paralysis Foundation and Alberta Heritage Foundation for Medical Research (AHFMR). W.F.C. and K.B. are Heritage Medical Scientists. We thank Vicky Staikopolis (University of Melbourne), Briana Napier and Araya Ruangkittisakul (University of Alberta) for technical advice and assistance, Helena Kim for carrying out the experiments with D.H.K. and Prof John Furness for access to confocal microscopy facilities at the University of Melbourne.

© 2009 The Authors. Journal compilation © 2009 The Physiological Society